OPTIMIZATION OF LAMELLA BURNER FIN DECK

A Thesis Submitted to
the Graduate School of Engineering and Sciences of
İzmir Institute of Technology
in Partial Fulfillment of the Requirements for the Degree of

MASTER OF SCIENCE

in Mechanical Engineering

by
Gökçe ÇETİN

July 2007
İZMİR

We approve the thesis of **Gökçe ÇETİN**

Date of Signature

…...…….. 12 July 2007
Prof. Dr. M. Barış ÖZERDEM
Supervisor
Department of Mechanical Engineering
İzmir Institute of Technology

…….. 12 July 2007
Prof. Dr. Zafer İLKEN
Co-Supervisor
Department of Mechanical Engineering
İzmir Institute of Technology

…….. 12 July 2007
Asst. Prof. Dr. Moghtada MOBEDI
Department of Mechanical Engineering
İzmir Institute of Technology

…….. 12 July 2007
Asst. Prof. Dr. Serhan KÜÇÜKA
Department of Mechanical Engineering
Dokuz Eylül University

…….. 12 July 2007
Assoc. Prof. Dr. Metin TANOĞLU
Head of Department
İzmir Institute of Technology

Prof. Dr. M. Barış ÖZERDEM
Head of the Graduate School

ACKNOWLEDGMENTS

I would like to express my appreciation to my supervisor Prof. Dr. Barış Özerdem and my co-supervisor Prof. Dr. Zafer İlken for their valued supports and comments throughout this study. I would like to acknowledge to Dr. Ing. Jörg Bruns, group leader in BBT Development Department, Manisa, for his comments and endless patience to my questions during this study; and to Dr. Ing. Heinz Bernd Grabenhenrich, head of BBT Development Department, Manisa, for the opportunity to use all the resources of the department for this study. I would like to thank also specially to Asst. Prof. Dr. Aytunç Erek, Dokuz Eylül University Department of Mechanical Engineering, Servet Yıldırım, Mustafa Ali Çakmak and all employees in BBT Development Department, Manisa.

ABSTRACT

OPTIMIZATION OF LAMELLA BURNER FIN DECK

Lamella burner is a low NOx burner patented by BOSCH Thermotechnologies. In this study, different designs of fin deck, which is one of the major components of the lamella burner, are experimentally analyzed and optimized. After the optimization process, a numerical analysis was used for verification.

Emissions are the most important properties for the gas fired boilers and directly related with the design of the burner parts where the combustion occurs. In the lamella burner, fin deck is the most related part with combustion. Combustion occurs on the fin deck surface hence, current fin deck design analysis and optimization is based on the emission rates in order to keep the lamella burner as low-emission (both NOx and CO) burner.

This study mainly consists: summary of main parameters regarding combustion and fin deck, experimental analysis, and verification of optimized fin deck model with numerical simulation. Firstly, gas combustion and lamella burner are investigated. Physical conditions and combustion characteristics for fin deck are analyzed and layout parameters for fin deck are deducted. Afterwards, four new fin deck designs are introduced as alternatives for the current design. In the experimental part, emission, light back, flame lift, temperature and pressure drop tests are performed for serial and each new sample in the BOSCH Product Development Laboratories, Manisa. According to the test results, the most preferred sample is defined as optimized one.

Test results are discussed to explain whether the fin deck samples are preferable or not. In the combustion curve performance test, CO values are measured. The comparison between the combustion curve test results show that CO formation is related to the fin deck geometry. Geometry affects flame stability because of the differences in mixture velocity distributions. The unburned gas in exhaust is one of the causes of the CO formation and influenced from the flame stability. Therefore, unburned gas mass fractions in exhaust are different for the samples with different geometries. This result is also numerically verified in combustion simulations of two different fin deck models, which one of them is considered as optimized sample.

ÖZET

LAMELLA BRÜLÖR KANAT DEMETİNİN OPTİMİZASYONU

Lamella brülör, BOSCH ısıtma teknolojileri patentli düşük NOx emisyonlu bir brülördür. Bu çalışmada, lamella brülörün başlıca parçalarından biri olan kanat demetinin farklı tasarımlarının deneysel analizi ve optimizasyonu yapılmıştır. Bazı deney sonuçları nümerik analizle doğrulanmıştır.

Emisyon oranları, yanmanın oluştuğu yüzey tasarımından doğrudan etkilenen bir özelliktir. Lamella brülörde yanma, kanat demeti yüzeyinde oluşur. Bu sebeple, lamella brülör kanat demeti tasarımının analizi ve optimizasyonu, emisyon oluşumunun (CO ve NOx ölçümlerine göre) düşürülmesi esasına dayanmaktadır.

Bu çalışma, lamella brülör kanat demeti özelliklerinin incelenmesi, deneysel analizi ve modelleme ile desteklemesi olmak üzere başlıca üç bölümden oluşmaktadır. İlk bölümde, gazların yanması, emisyonlar, gaz brülörleri ve düşük emisyonlu lamella brülör incelenmiştir. Sonrasında kanat demeti ile ilişkili fiziksel özellikler ve yanma karakteristikleri analiz edilmiştir. Bu analize dayanarak kanat demeti yapısal parametreleri bir araya getirilmiştir. Ardından kullanımdaki tasarıma alternatif olarak dört kanat demeti tasarlanmıştır. Bu alternatif tasarımlar birbirlerine ve kullanımdaki tasarıma göre kanat kalınlıkları, uzunlukları ya da üretim süreçleri bakımından farklıdırlar. Deneysel analiz bölümünde, her bir yeni tasarım ve kullanımdaki kanat demeti için BOSCH Manisa Geliştirme Laboratuarı'nda emisyon, alev kararlılığı (geri tepme ve alev kopması), sıcaklık ve basınç kaybı testleri yapılmıştır. Test sonuçları karşılaştırılarak optimum kanat demeti tasarımı belirlenmiştir.

Sonuç olarak bu çalışmada, lamella brülör kanat demeti ve dört yeni tasarımı test edilmiş, sonuçları karşılaştırılmış ve sonuçların teorik açıklamaları yapılmıştır. Emisyon testlerinde farklı CO miktarları ölçülen iki yeni tasarım karşılaştırılmış ve geometrideki farkların alev kararlılığını, bu yüzden de egzozdaki yanmayan gaz miktarını etkilediği görülmüştür. Bu iki tasarım modellenmiş ve egzoz simülasyonlarındaki kütlesel metan oranları karşılaştırılmıştır. Deney sonuçlarıyla karşılaştırılan nümerik modelleme sonuçları geometrinin alev kararlılığına etkisini doğrulamıştır.

TABLE OF CONTENTS

LIST OF FIGURES

LIST OF TABLES

NOMENCLATURE

a	injection distance [m]
A	area [m^2]
c_p	specific heat [kJ/kg·K]
d	flow diameter, fin to fin distance (for lamella burner fin deck) [mm]
$D_{i,m}$	diffusion coefficient for species i in mixture [m^2/s]
h	specific enthalpy [kJ/kg]
h_f^o	formation enthalpy [kJ/kg]
H	calorific value [kJ]
H_s	higher calorific value [kJ]
$\dot{I}$	momentum rate [N]
k_f	conductivity of fluid [W/m·K]
K	mixing duct/burner coefficient
$\dot{m}$	mass flow rate [l/s]
P	pressure [Pa]
R_i	mass rate of creation or depletion by chemical species i
S_L	laminar flame velocity [m/s]
T	temperature [K]
u	axial mean velocity [m/s]
v	velocity [m/s]
V_x	velocity in x direction [m/s]
V_y	velocity in y direction [m/s]
$\dot{V}$	volumetric flow rate [kg/s]
W	Wobbe index
Y_i	local mass fractions of species i

Greek Symbols

λ	excess air ratio
μ	molecular viscosity [m^2/s^2]
ρ	density [kg/m^3]
τ_{ij}	stress tensor [N/m^2]

Φ	equivalence ratio
ξ	loses

Subscript

ad	adiabatic
g	gas
i	initial state
u	unburned

CHAPTER 1

INTRODUCTION

1.1. Gas Combustion

Combustion is an exothermic chemical reaction, which occurs by breaking down a substance with oxygen. This process is called as oxidation and categorized with respect to reaction times as slow and rapid oxidation. When oxidation takes place in very long time, there will be little production of heat and no production of light. It is observed in corrosion, and the main difference between the processes of corrosion and combustion is the amount of heat production. Since combustion is completed in a rapid oxidation, there is heat generation at a high temperature. Therefore, generated heat in combustion is useful for heating processes.

Oxygen is the main requirement for combustion, and the substance, which serves the need of oxygen, is called as oxidizer. In almost every gas combustion process, the oxidizer is air. Flammable gas mixes with air, called aeration, either before or during the burning process. These two situations are called as premixed combustion and non-premixed combustion, respectively. Premixed combustion occurs in two ways as being fully and partially. In fully premixed systems, the entire amount of required air is provided and mixed with fuel prior to the combustion reaction. The difference of partially premixed systems is that the reactants mix both before and during the chemical reaction. In non-premixed combustion, fuel and air are initially separated, and combustion occurs only at the interface between them diffusing the fuel and oxidizer molecules toward the flame from the opposite directions.

The amount of oxygen in combustion process is also an important criterion. It determines the quality of combustion reaction. If fuel burns with required amount of oxygen, which is determined relative to the amount of fuel, there will be produced the main combustion products. This type of combustion process is called as complete combustion and the combustion products are CO_2 and H_2O. If less than the required amount of oxygen is supplied, fuel will not burn completely. In such an incomplete combustion, some miner compounds will be produced in addition to the main combustion products.

There are complete combustion reactions of some flammable gases below (Cerbe 1999).

$$H_2 + \tfrac{1}{2} O_2 \rightleftharpoons H_2O$$

$$CO + \tfrac{1}{2} O_2 \rightleftharpoons CO_2$$

$$CH_4 + 2\ O_2 \rightleftharpoons CO_2 + 2\ H_2O$$

$$C_2H_4 + 3\ O_2 \rightleftharpoons 2\ CO_2 + 2\ H_2O$$

$$C_2H_6 + \tfrac{7}{2} O_2 \rightleftharpoons 2\ CO_2 + 3\ H_2O$$

$$C_3H_8 + 5\ O_2 \rightleftharpoons 3\ CO_2 + 4\ H_2O$$

$$C_4H_{10} + \tfrac{13}{12} O_2 \rightleftharpoons 4\ CO_2 + 5\ H_2O$$

Generally;

$$C_xH_y + (x + \frac{y}{4})\ O_2 \rightleftharpoons x\ CO_2 + \frac{y}{2}\ H_2O$$

Air is used as an oxidizer in most combustion processes, since it is easy to supply from atmosphere into the burning system without any cost. Simplified composition of air is assumed 21 percent O_2 and 79 percent N_2 (by volume). In chemical meaning, there are 3.76 moles of N_2 for each mole of O_2 in air. When air is the oxidizer, the general combustion equation transforms into the below equation.

$$\underbrace{C_xH_y + (x + \frac{y}{4})\ (O_2 + 3.76\ N_2)}_{\text{Theoretical Air Requirement}} \rightleftharpoons x\ CO_2 + \frac{y}{2}\ H_2O + 3.76\ (x + \frac{y}{4})\ N_2$$

The **theoretical air requirement** is the stoichiometric quantity of air, which is precisely required amount of air as an oxidizer for a complete combustion. The air quantity in the real combustion processes could not be always equal to theoretically required amount of air. If more than the stoichiometric quantity of air is supplied, the mixture is called as being fuel-lean; and the mixture is said to be fuel-rich in the opposite situation.

For premixed system, it is also important to define the primary air quantity in a combustion process. It is expressed as the **primary aeration ratio, λ,** and shows how much air is premixed with gas before combustion.

$$\lambda = \frac{volume\ of\ \ primary\ air}{theoretical\ air\ requirement\ (by\ volume)} \tag{1.1}$$

In gas combustion, gas type is also important since the amount of its C and H molecules directly designates the theoretical air ratio and λ. In addition, there are many different types of flammable gases, which have their own physical and chemical properties. All of the properties make the gas affect to the combustion process in many ways like emissions, energy production, etc., and can be called as burning behavior of a gas.

The **Wobbe index** is one of the most important gas properties, since the produced energy of a gas is linearly proportional to its Wobbe index. Therefore, flammable gases are divided into three families based on their Wobbe numbers. It is defined as the ratio of the higher calorific value (H_s) to the square root of the relative density to air (ρ).

$$W = \frac{Hs}{\sqrt{\rho}} \tag{1.2}$$

Hs : higher calorific value, d : relative density to air

Roughly, the gases related to the same gas family show same burning behavior. The general properties of three gas families are represented in Table 1.1.

Table 1.1. Properties of the gas families

	Type of gas	**Wobbe Index**	**Main Component**	**Relative Density**
First gas family	Manufactured Gases - Town Gas	20 - 40 MJ/m^3	Hydrogen	0,45 - 0,65
Second gas family	Natural Gases	40 - 75 MJ/m^3	Methane	0,60 -0,65
Third gas family	Liquified Petroleum Gases	75 - 90 MJ/m^3	Propane - Butane	1,5 - 2,0

1.2. Emissions

1.2.1. Main Combustion Products

Some combustion products are the main components of combustion process. These products are CO_2 and H_2O that are typical products of complete combustion.

CO_2 is a harmful compound, since it contributes to the greenhouse effect, which changes the climatology, for example, it causes global warming. CO_2 may also be detrimental to human health at high levels. H_2O is the other main constituents of combustion products. H_2O is not considered harmful to human or environment.

In addition, N_2 is also found in exhaust gas with the main combustion products, when the oxidant O_2 is getting from air. The big amount of the N_2 concentration comes from the air, and the rest may come from the flammable gas.

1.2.2. NO_x Emissions

Oxides of nitrogen, NO_x, consist of NO and NO_2. NO is an important minor component of combustion process, which causes air pollution. In the atmosphere, NO_2 is formed from the oxidation of NO, which is also important because of its effect on the acid rain and photochemical smog productions.

NO is the primary nitrogen oxide from combustion systems. NO_2 is usually produced because of NO to NO_2 conversion of non-premixed systems in low temperatures. Nitric oxide is formed by thermal (Zeldovich) mechanism, prompt (Fenimore) mechanism and N_2O-intermediate mechanism.

The **thermal** or **Zeldovich mechanism** dominates at high temperatures in combustion over a wide range of primary aeration ratios. This mechanism consists of two chain reactions as (1.3) and (1.4).

$$O + N_2 \rightleftharpoons NO + N \quad (1.3)$$

$$N + O_2 \rightleftharpoons NO + O \quad (1.4)$$

The extended Zeldovich mechanism is formed by adding the reaction (1.5).

$$N + OH \rightleftharpoons NO + H \quad (1.5)$$

Thermal NO is found mainly in the high-temperature exhaust gases. The thermal mechanism is generally coupled to the combustion through O_2 (Fig. 1.1), O and OH species. The nascent oxygen atom in equation (1.4) is from the H_2-O_2 radical pool or dissociation of O_2. Dissociation is a reaction can that can be observed as reverse combustion. At high flame temperatures, some of the combustion products reabsorb the combustion energy and break down. OH radical in equation (1.6) come possiblely from the following reaction, which obtains the hydrogen atom from the dissociation of hydrocarbon fuel (WEB_2 2000).

$$H + O_2 \rightleftharpoons OH + O \quad (1.6)$$

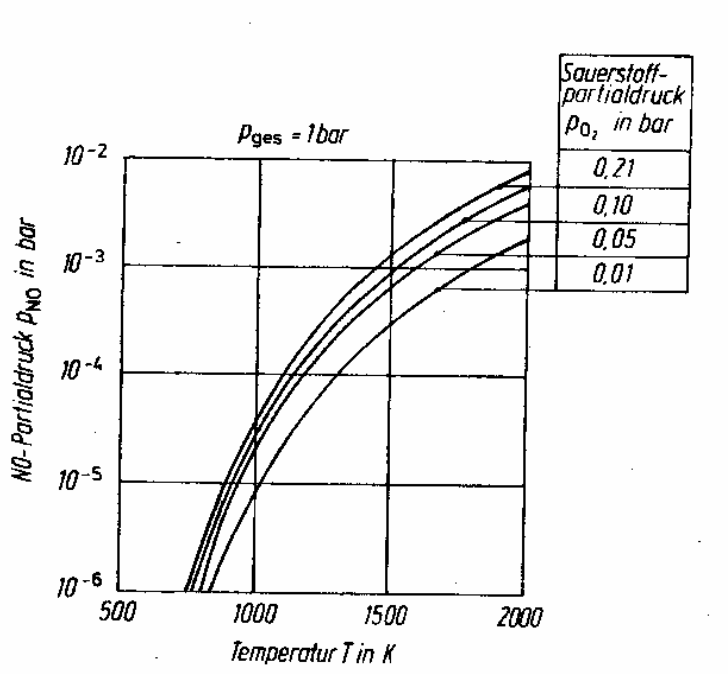

Figure 1.1. NO and O_2 partial pressures as a function of temperature.
(Source: Cerbe 1999)

The thermal NO mechanisms react in both equilibrium and superequilibrium phases. Their contributions in the fraction of total NO formations are shown in Table 1.2.

The Fenimore or prompt mechanism considers the mechanism of rapid NO production, and it is linked to the combustion of hydrocarbons. It was found by

Fenimore that some NO was rapidly produced in premixed laminar flames long before the thermal NO production. The prompt mechanism can be written as the following chain reactions (1.7) and (1.8) initiating that after the CH formation (Turns 2000).

$$CH + N_2 \rightleftharpoons HCN + N \quad \text{(the primary path)} \qquad (1.7)$$

$$C + N_2 \rightleftharpoons CN + N \qquad (1.8)$$

For $\lambda > 0.8$, the conversion of HCN to NO is like following chain sequence:

$$HCN + O \rightleftharpoons NCO + H \qquad (1.9)$$

$$NCO + H \rightleftharpoons NH + CO \qquad (1.10)$$

$$NH + H \rightleftharpoons N + H_2 \qquad (1.11)$$

$$N + OH \rightleftharpoons NO + H \qquad (1.12)$$

For $\lambda < 0.8$, the NO is recycled to HCN. Thus, NO formation is inhibiting, and the mechanism is no longer rapid.

The **N_2O-intermadiate mechanism** is important for $\lambda > 1.25$ and in low temperatures especially for NO control strategies in fully premixed combustion.

$$O + N_2 + M \rightleftharpoons N_2O + M \qquad (1.13)$$

$$H + N_2O \rightleftharpoons NO + NH \qquad (1.14)$$

$$O + N_2O \rightleftharpoons NO + NO \qquad (1.15)$$

1.2.3. CO Emissions

CO is the other important minor component of the combustion process and harmful to human health or even fatal at levels over 1000 ppm. When CO is breathed, it displaces oxygen in the blood and reduces the needed oxygen for heart, brain, and other vital organs. Large amounts of CO can overload the body in minutes without warning and causes to loose consciousness and suffocate. There is shown the effects CO exposure on humans in Figure 1.2.

Table 1.2. Relative contributions of various mechanisms to NO_x formation in laminar premixed flames (Source: Turnes 2000).

λ	P (atm)	Total NO_x (ppm)	Fraction of Total NO Formation			
			Equilibrium Thermal	Superequilibrium	HC-N_2	N_2O
1	0.1	9	0,04	0,22	0,73	0,01
1	1.0	111	0,50	0,35	0,10	0,05
1	10	315	0,54	0,15	0,21	0,10
0.95	1	29	0,53	0,30	0,17	-
0.86	1	20	0,30	0,20	0,50	-
0.78	1	20	0,05	0,05	0,90	-
0.76	1	23	0,02	0,03	0,95	-

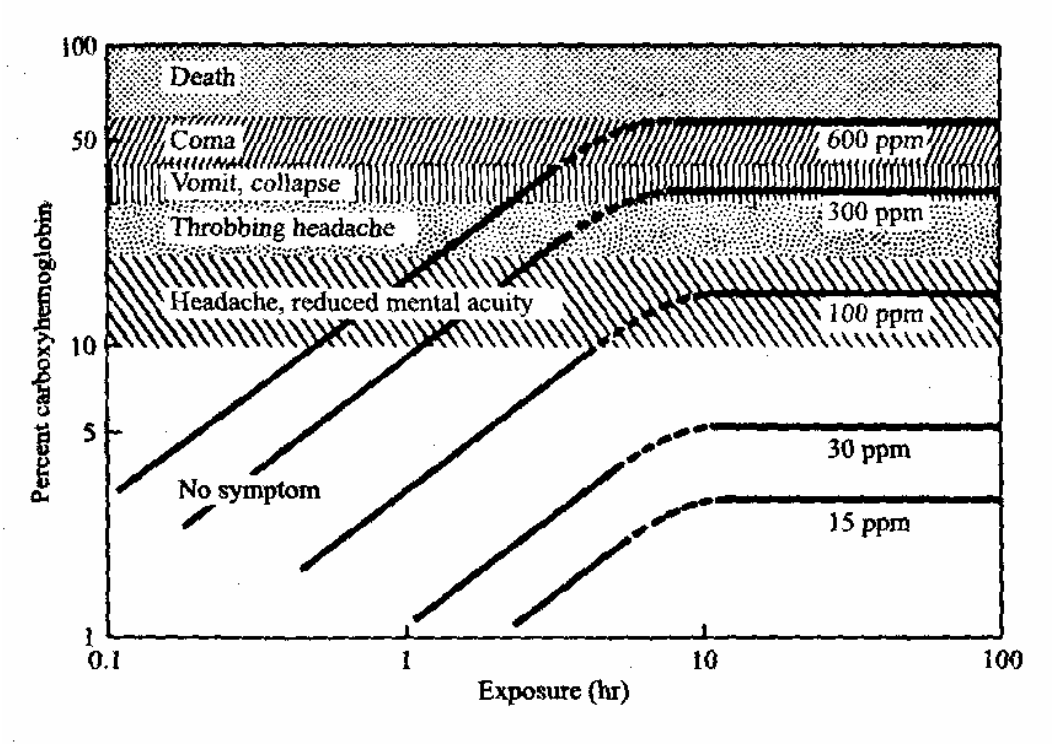

Figure 1.2. Effects of CO exposure on humans.
(Source: Turnes 2000)

CO is an inevitable combustion product whenever fuel-rich mixtures are used in combustion. In fuel-rich combustion processes, there will be observed incomplete combustion and unburned hydrocarbon molecules. Only about a third of the unburned hydrocarbons are found in exhaust as fuel molecules. The partial combustion of remain hydrocarbons results CO production (Turnes 2000).

For the stoichiometric and fuel-lean mixtures, CO is found in substantial quantities at adiabatic flame temperatures (2033K - 2260K) as a result of dissociation of CO_2.

$$CO + ½\ O_2 \rightleftharpoons CO \qquad (1.16)$$

In Figure 1.3, the upper curve shows CO concentrations in the product gases of adiabatic, atmospheric-pressure, propane-air flames. The lower curve shows the values for equilibrium at a temperature of 1500 K.

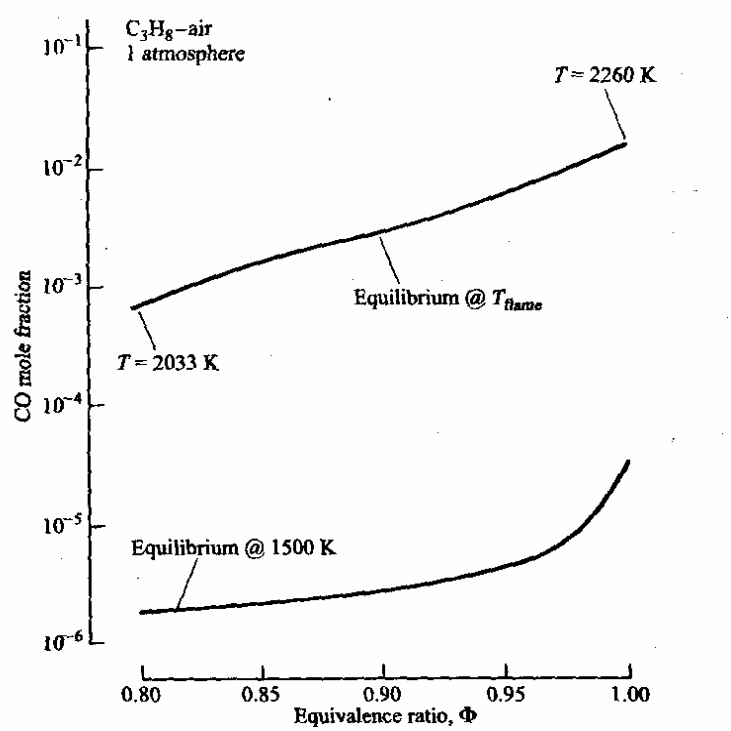

Figure 1.3. Equilibrium CO mole fractions in propane-air combustion products at adiabatic flame temperatures and at 1500 K (Source: Turnes 2000).

1.3. Gas Burners

Burners are heat production components, which set the chemical energy of a combustion reaction by

- supplying gas and air (as flammable substance and oxidizer),
- mixing them,
- igniting the gas-air mixture and stabilizing the combustion reaction.

Burners for gas heating appliances provide defined conditions for the combustion process in order to achieve a high usage of energy and low emission rates, and they are classified into two classes as **fan assisted** and **atmospheric** burners according to their air supplying and gas-air mixing systems. They can furthermore be classified into **partially premixed** and **fully premixed** burners according to their flame types.

1.3.1. Fan Assisted Gas Burners

In this kind of burners, air is supplied by a fan, blower or compressor. Then gas is piped to the fan's inlet to let it mix gas with air, and then fan pushes the mixture into the burner (Figure 1.4). The equipment is also called as fan mixer. Fan assisted burners are generally used in industrial burners and in condensing appliances.

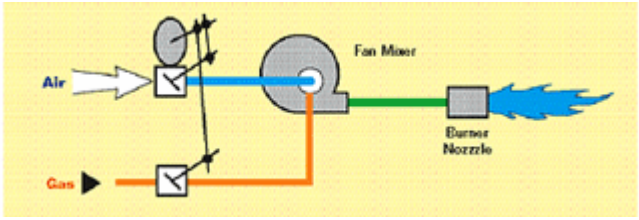

Figure 1.4. Fan mixer.
(Source: WEB_3 2003)

In fan assisted burners, gas and air are supplying by the same device but from different entrances. Therefore even small changes in any flow influence the other flow inversely and it becomes important to use gas/air ratio control, which ensures that the gas-air ratio remains constant especially in any changes of gas pressure.

1.3.2. Atmospheric Gas Burners

In atmospheric burners, air is supplied and mixed with gas naturally. There is no auxiliary energy to carry air and mix with gas. Gas is injected at high velocities into the burner entrance, where the stationary air is found. Therefore shear forces between air

and gas jet cause air to be taken from burner's surroundings into the burner, and then gas and air mix in the burner's mixing chamber automatically.

Atmospheric burners are classified into two types as being partially and fully premixed depending on their aeration types. These have the same concept with premixed combustion systems mentioned about in the "gas combustion" part.

Partially premixed atmospheric burners supply the air needed for combustion in the form of both primary and secondary air. The amount of air, which is premixed with the gas, is normally expressed as a percentage of the theoretical quantity of air required for combustion, and is often referred to as the percentage primary aeration. Partially premixed burners generally operate within the range of 40-60% primary aeration. Namely, it can be also said that primary aeration ratio λ is less than one ($\lambda<1$) in this kind of burners. The rest need of air for a complete combustion is supplied as secondary air during the combustion reaction. This type of burner is widely used in the conventional gas appliances.

Fully premixed atmospheric burners supply at least all the theoretically required amount of air for a complete combustion in the form of primary air ($\lambda\geq1$). The primary aeration ratio, λ is bigger than one in the combustion process of fuel-lean mixtures.

Before defining the primary aeration concept in atmospheric burners, it is important to investigate the mass flow rate in the unrestricted aeration which is the aeration of a free gas jet. Investigation of the unrestricted aeration constitutes the basis of the aeration of atmospheric burners.

There is illustrated an unrestricted aeration, which has no obstruction in front of the gas injector, in Figure 1.5. Gas spreads out the nozzle adding the surrounding air to the flow. In such a flow, the average gas/air ratio can be defined estimating the initial and final mass flow rates. The initial and final variables are shown as the variables at the point 0 and x1, respectively.

In the experimental analysis, an angle between 18 - 20 degrees has been defined for the cone shape jet flow. After the distance x from the injector outlet, cone diameter d_x can be defined as in equations (1.17) and (1.18).

$$d_x = 2\,(x + a)\tan\frac{\gamma}{2} \tag{1.17}$$

$$d_x = 0.322\,(x + a) \quad \text{,where } \gamma = 18 \text{ to } 20^\circ \tag{1.18}$$

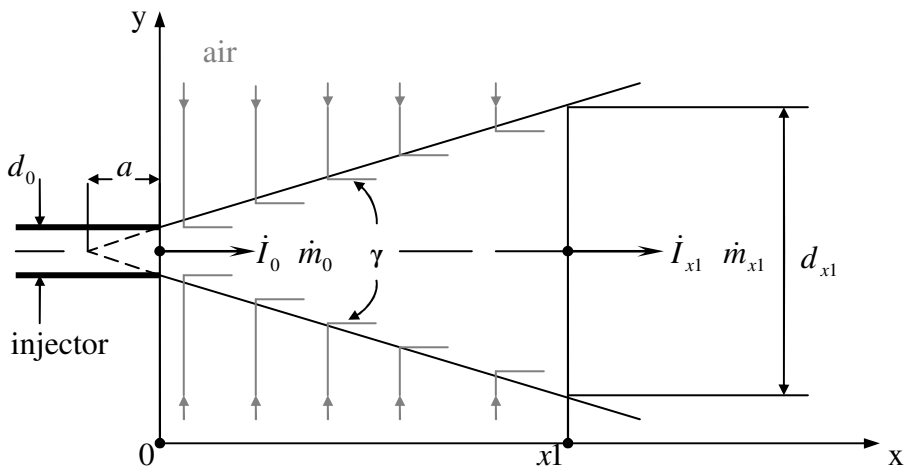

Figure 1.5. Unrestricted aeration.

(Source: Cerbe 1999)

Conservation of the momentum is used to reach the ratio of mass flow rates at $x = 0$ and $x = x1$.

$$\dot{I}_0 = \dot{I}_{x1} \tag{1.19}$$

$\dot{I} = \dot{m}\ v$ (1.20), where v is the velocity at the center of the cone cross-section. Introducing the equation (1.20) for 0 and x1 points into the equation (1.19), equation (1.21) is defined.

$$\dot{m}_0\, v_0 = \dot{m}_{x1}\, v_{x1} \tag{1.21}$$

$$\dot{m} = \rho\, v\, \frac{\pi d^2}{4} \tag{1.22}$$

Using the equations (1.21) and (1.22), equation (1.23) is derived.

$$\frac{v_0}{v_x} = \frac{d_{x1}}{d_0} \sqrt{\frac{\rho_{x1}}{\rho_0}} \tag{1.23}$$

According to the definitions, the ratio of mass flow rates are as below accepting $x1 >> a$:

$$\frac{\dot{m}_{x1}}{\dot{m}_0} = 0.322\ \frac{x1}{d_0} \sqrt{\frac{\rho_{x1}}{\rho_0}} \tag{1.24}$$

The fraction of mass flow rates of gas and air can be defined as the fraction of volumetric flow rates using the equation $\dot{V} = \dot{m} / \rho$ as:

$$\frac{\dot{V}_{x1}}{\dot{V}_0} = 0.322 \ \frac{x1}{d_0} \sqrt{\frac{\rho_0}{\rho_{x1}}} \tag{1.25}$$

The variables at the point 0 define the pure gas properties and can be represented as:

$$\dot{V}_0 = \dot{V}_g \quad \text{and} \quad \rho_0 = \rho_g \tag{1.26) (1.27}$$

Density and volumetric flow rate of the gas-air mixture at the point $x1$ can be also defined as the equations (1.28) and (1.29).

$\rho_{x1} = \rho_{mix}$ (1.28) and $\dot{V}_{x1} = \dot{V}_g + \dot{V}_a$ (1.29), where $\dot{V}_a$ is the volumetric flow rate of air.

Then, the fraction of volumetric flow rates of gas and mixture becomes:

$$\frac{\dot{V}_g + \dot{V}_a}{\dot{V}_g} = 0.322 \ \frac{x1}{d_0} \sqrt{\frac{\rho_g}{\rho_{mix}}} \tag{1.30}$$

$$\frac{\dot{V}_a}{\dot{V}_g} = 0.322 \ \frac{x1}{d_0} \sqrt{\frac{\rho_g}{\rho_{mix}}} \ - 1 \tag{1.31}$$

Due to $\dot{m}_g << \dot{m}_a$ at the point $x1$, the gas density in the mixture can be neglected, and the equation for unrestricted aeration becomes as the equation (1.32).

$$\frac{\dot{V}_a}{\dot{V}_g} = 0.322 \ \frac{x1}{d_0} \sqrt{\frac{\rho_g}{\rho_a}} \ - 1 \tag{1.32}$$

In Figure 1.6, there is shown the gas injection in a mixing duct, which causes primary aeration of an atmospheric burner. There is only one difference from unrestricted aeration; the jet is restricted with the inner shell of the mixing duct.

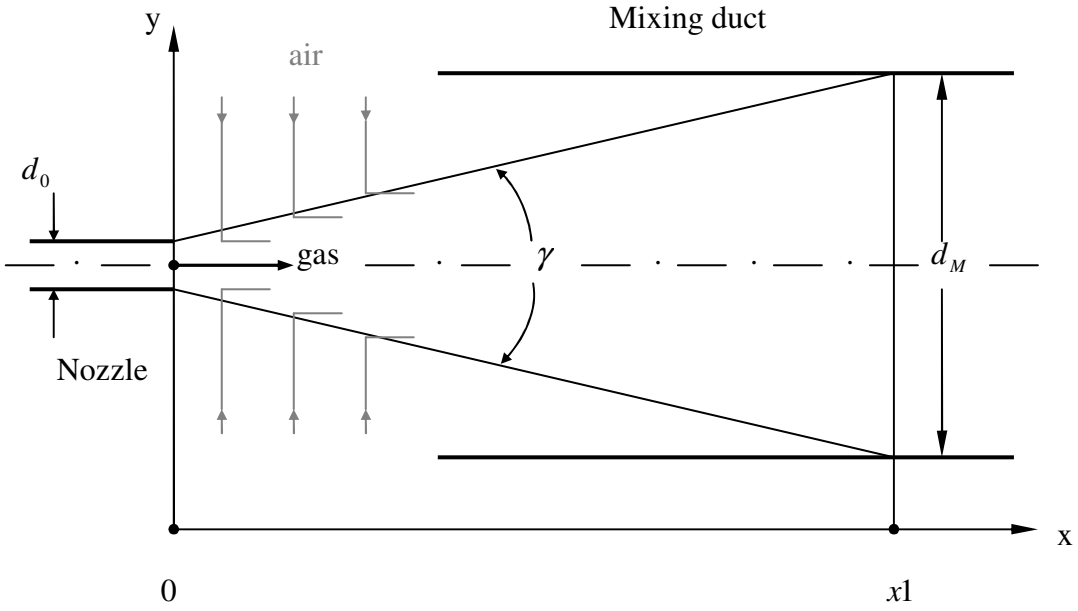

Figure 1.6. Primary aeration of an atmospheric burner.

The formula for calculating air entrainment in an atmospheric burner is derived with the same logic as for the unrestricted aeration taking additionally temperature influences and the flow resistance of the mixing duct/burner into account.

$$\frac{\dot{V}_a}{\dot{V}_g} = \frac{d_M}{d_0} K \sqrt{\frac{\rho_g}{\rho_a} \frac{T_{amb}}{T_m}} - 1 \tag{1.32}$$

, where K : Burner/mixing duct coefficient

T_{amb} : absolute temp of the ambient air

T_m : mean absolute temperature in the mixing tube/burner head.

From this equation, the primary air ratio λ can be calculated using $Theoretical\ Air\ Ratio = \dot{V}_g\ (x + \frac{y}{4})\ 4.76$ and substituting it into the equation (1.1)

$$\lambda (x + \frac{y}{4}) 4.76 = \frac{\dot{V}_a}{\dot{V}_g} \tag{1.33}$$

Finally, the primary aeration ratio of an atmospheric burner can be defined using the equations (1.32) and (1.33) as the equation (1.34)

$$\lambda = \frac{1}{(x+\frac{y}{4})4.76}\left(\frac{d_M}{d_0} K \sqrt{\frac{\rho_g}{\rho_a}\frac{T_{amb}}{T_m}} - 1\right) \tag{1.34}$$

1.3.3. Emissions and EU Standards for Atmospheric Burners

Emissions are very important properties of the burners, and there is a tendency to compare burners with respect to their emission rates. NO_x and CO rates of a combustion process determine the burner characteristics about whether to be harmful for the human health and environment or not.

There are some applications done to reduce the emission rates. Cooling the flame touching surface is a method to reduce the NO_x emission rate. NO_x are intensively forming at high temperatures as defined in the thermal NO_x mechanism in part 1.2.2. Cooling the combustion surface provides flame temperatures not to get higher. The burners, which reduced the NO_x emission rates, are called as "Low-NO_x burners". In this type of burners, water cooling is generally used to reduce the NO_x emissions (there are some applications with air cooling).

Exhausts, which are formed in combustion, are yielded into the atmosphere. The emission rates are restricted in order to prevent human health and environment. The allowed maximum CO and NO_x rates are defined in EU Standards (The European Standard EN 297:1994 2003, The European Standard EN 483:2000 2002). These limitations are valid under defined test and calculation conditions, which will be described in details in Chapter 4. Generally, the CO content of dry and air free combustion products shall not exceed 1000 ppm, when the boiler is supplied with the reference gas under the normal or special conditions or 2000 ppm, when the boiler is supplied with the incomplete combustion limit gas. As for NO_x content, there are defined five NO_x class of the boiler. The permissible NO_x concentrations for each class are listed in Table 1.3.

Table 1.3. Limit NO_x concentrations to define the NO_x classes according to EN 297.

NO_x Classes	Limit NO_x concentration in mg/kWh
1	260
2	200
3	150
4	100
5	70

1.4. Low-NO_X-Lamella Burner

The Low-NO_x-Lamella Burner is a fully premixed atmospheric burner constructed by BOSCH Thermotechnologies. The main characteristics of the Lamella Burner can be defined as being;

- horizontal nozzle system,
- shared mixing chamber,
- water cooled fin deck.

The function of the lamella burner can be summarized as below.

- Gas coming from the gas valve enters the gas distribution tube via one connection on the side (for easy serviceability) and exits through a set of nozzles.
- From each nozzle, the gas enters into the horizontal mixing ducts of the mixing chamber, where complete mixture occurs with air by the help of the gas momentum.
- The mixture is combusted on the combustion surface after passing the water cooled fins.

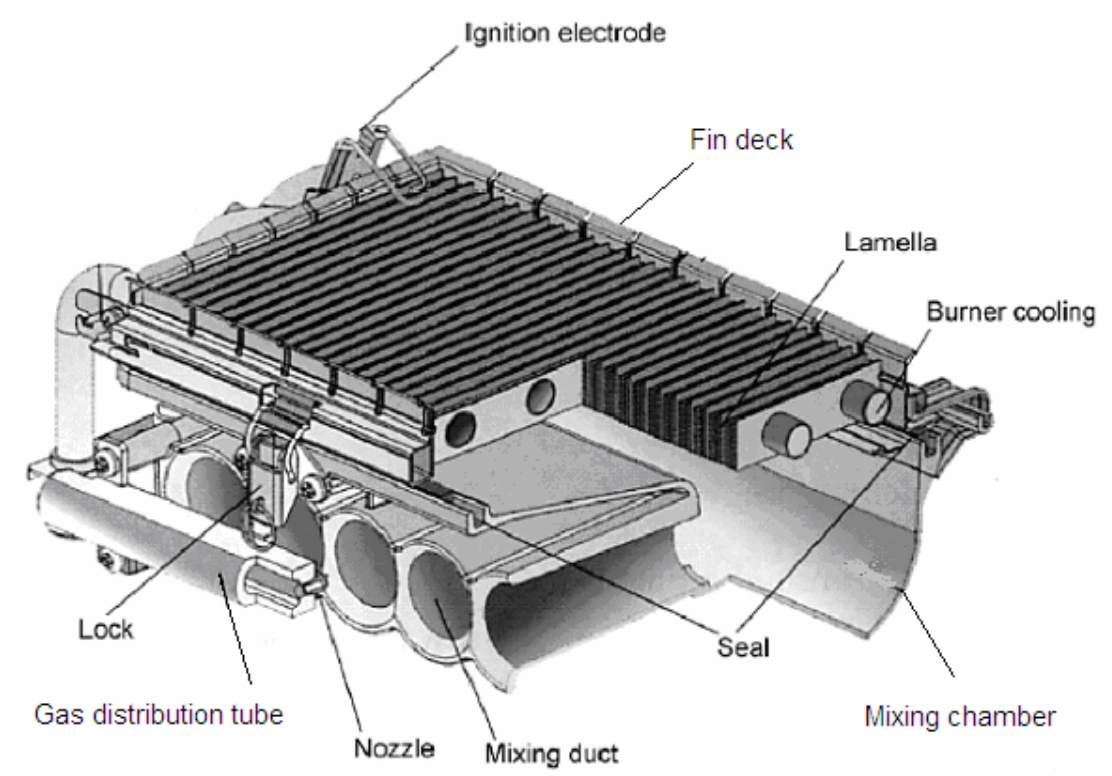

Figure 1.7. Low NO_X lamella burner.

Lamella burner has three different versions according to the heat outputs of the appliances. There are 11 kW (4 mixing ducts), 18 kW (6 mixing ducts) and 24 kW (8 mixing ducts) lamella burners. Lamella burner width increase with increasing heat output, the other dimensions stay constant.

1.4.1. Main Parts of the Lamella Burner

Gas distribution tube is the connection part of the Lamella Burner with the gas way. It provides gas distribution into the mixing chamber with the mounted nozzles. It is fixed toward the entrance of the mixing ducts leaving some space. The distance between the gas distribution tube and mixing duct entrance is definitely critical dimension, since it has to allow enough primary air access in to the burner.

Mixing chamber is formed from horizontal mixing ducts and a chamber, into which all the ducts are opening. It is produced as a single part by Alu-casting. It was designed to guide the gas-air mixture to the combustion surface and allow mixing them homogeneously.

During the gas injection, air is supplying by shear forces into the mixing ducts. Gas and air pass through the ducts together and start to mix there. After the mixing ducts, the gas-air mixture is deflected 90° by a smooth radius in order to keep pressure drop on the gas side low. After this 90° bend, there is placed a perforated sheet metal, called as baffle and made from steel, in order to provide an even distribution of the gas-air mixture on the combustion surface (Figure 1.8).

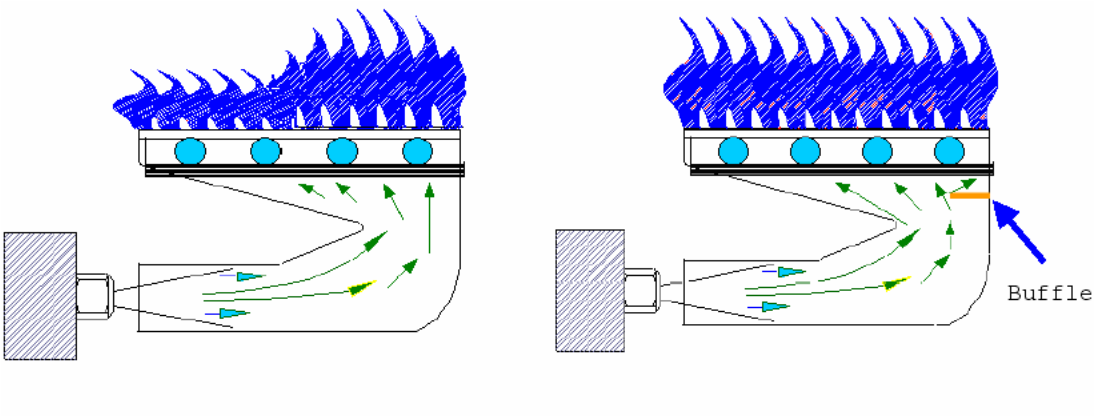

Figure 1.8. Flame distribution with and without buffle.
(Source: Plothe and Sönmezışık 2003)

Fin deck is the upper part of the lamella burner, where combustion occurs. It is formed from different parts; mainly, copper tubes, fins, frame and collar. In the frame, fins are stringed to the copper tubes, in which cooling water flows in order to reduce fin temperature. Fins are connected also to the frame by welding. Welding provides the mechanical stability and the heat transfer from the frame to the fins. Collar surrounds the upper side of fins to prevent secondary air access, and it is fixed to the frame. The collar has numerous vertical cuts to minimize its thermal tension and hence in order to prevent bending or crackling noise (Figure 1.9). The cuts are small enough (1mm) not to let any significant amount of secondary air through.

There are some accessories on fin deck like ignition electrode and ionization electrode. Ignition electrode sets fire to the gas air mixture and ionization electrode checks the flame existence on the combustion surface.

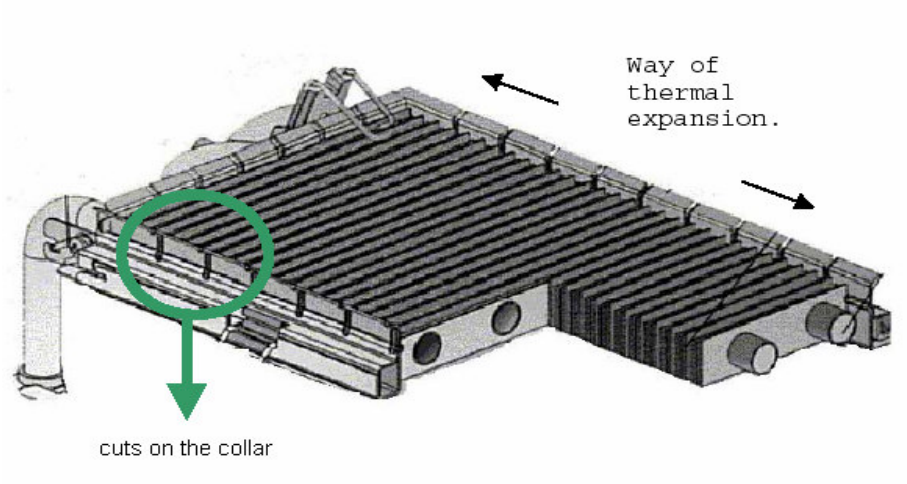

Figure 1.9. Lamella burner fin deck.

(Source: Plothe and Sönmezışık 2003)

Fin deck fits on the mixing chamber. The gas-air mixture coming from mixing chamber passes through the water cooled fins. Combustion occurs on the top surface of the fin deck by igniting the gas air mixture. Flames are touching to the fin tips and therefore cooled. Fins are arranged as being 2 - low and 1 - high (Figure 1.10).

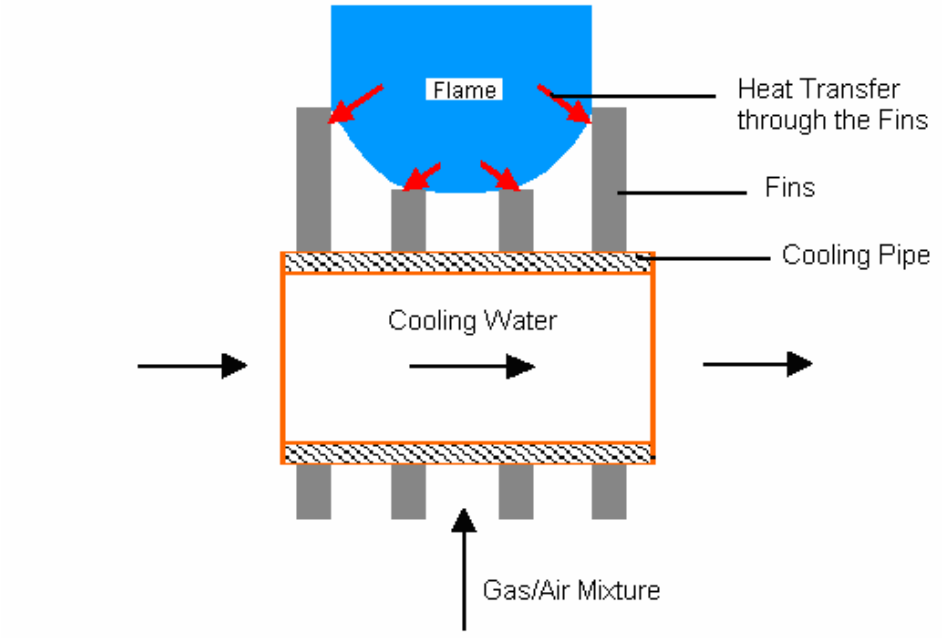

Figure 1.10. Flame cooling.

Fin deck and mixing chamber are connected by fasteners providing sufficient force to achieve gas side soundness. Therefore fin deck and mixing chamber are allowed to expand independently from each other, and there occurs no thermal stress on the burner body. These quick release fasteners provide also easy servicing, which is an important marketing argument about simple assembly / disassembly (Figure 1.11).

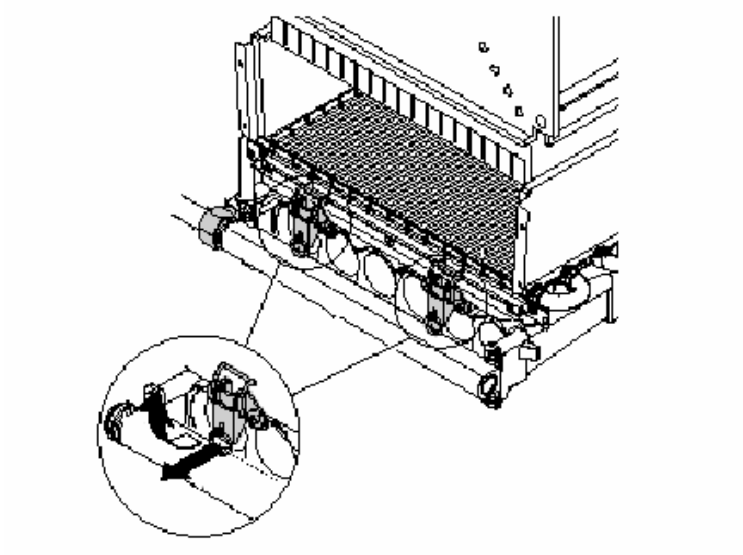

Figure 1.11. Easy servicing (fasteners).
(Source: Plothe and Sönmezışık 2003)

There is a rubber sealing between the fin deck and mixing chamber. The sealing touches the fin deck frame and mixing chamber and obstacles the leak of gas air mixture out of the burner.

1.4.2. Integration of the Lamella Burner into the Appliance

Lamella burner is integrated into appliance by way of the gas and water connection. Lamella burner is connected to the hydraulic system with the cooling pipes of the fin deck. Gas connection of the lamella burner is between the gas distribution tube and the gas valve. The connection with the gas way is on the side of gas distribution tube. It allows easy assembly/disassembly of the mixing chamber only opening the gas connection (Figure 1.12).

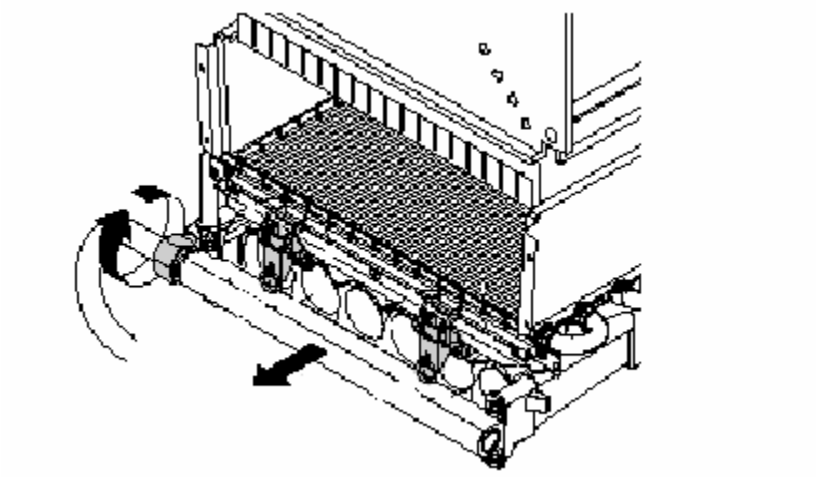

Figure 1.12. Easy servicing (gas connection).

(Source: Plothe and Sönmezışık 2003)

CHAPTER 2

LITERATURE SURVEY

Emission control in gas fired appliances is recently getting more important owing to the environmental regulations about emission reductions in exhaust gases. Therefore, low-NOx burner usages are increasing in combi boilers. Since combustion technology has been a popular topic for researchers for years and the requirement to significantly reduce NOx and particulate emissions while maintaining combustor performance is one of the main drivers for combustion systems, emissions have been investigated theoretically, experimentally and numerically in lots of studies.

Fuel composition is the one of the property affects emissions in combustion systems. The influence of fuel composition on emissions of CO, NO, and NO_2 from a gas-fired pulsed combustor has been investigated using a wide range of fuel flowrates and fuel compositions for a commercially available non-premixed pulsed combustion room heater (Jones and Leng 1996). It has been observed that NOx emissions increase as the fuel flowrate increased, when burning methane alone. Adding propane and small amount of hydrogen has increased also the NOx emissions by lowering the excess air in the combustion chamber and hence increasing the chamber temperature. In case of the hydrogen percentage in the fuel higher than 20% a sudden increase in the emission of CO, and a decrease in the emission of NOx has been observed owing to a reduction in temperature. Fuel effect on NOx emissions in partially premixed flames has been investigated by Naha and Aggarwal (Naha and Aggarwal 2004). This study has reported on the results of a numerical investigation on the effects of using fuels included methane, *n*-heptane, and their blends with hydrogen on NOx emissions in counterflow partially premixed flames. Results has been indicated that, with regard to their NOx characteristics, partially premixed flames can be grouped into two distinct regimes, namely a double-flame regime and and a merged-flame regime, characterized by levels of partial premixing and/or strain rates.

Fuel-air equivalence ratio is another property investigated in the studies about emissions. Local production rates of NO have been derived from experiments in vertical flames with the fuel-air equivalence ratio of around 1.9 on a burner commonly used in

central heating equipment (Dupont and Williams 1998). This equivalence ratio has caused a double flame structure and the production rate of NO has been maximum in regions of low temperature and low OH concentration, located in the inner premixed flame and prior the higher temperatures and OH concentrations of the outer diffusion flame. Experimental results have showed the main NO formation mechanism was the Fenimore Prompt route and an internal reburn mechanism. Chou at all has developed a numerical model for fast predictions of NOx and CO emissions from laminar flames and applied to studying NO formation in the secondary non-premixed flame zone of fuel-rich methane Bunsen flames (Chou et al. 1998). The computed results have been showed a decreasing trend of NOx emission with the equivalence ratio but an increasing trend in the CO emission index.

As it can be seen in some of the above mentioned studies, Bunsen burner is a common used device to construct the flame structure in researches. Bunsen burner was invented by German chemist Robert Wilhelm Bunsen. Although it is named after his invention, it is actually an improvement made in 1855 by his laboratory assistant, Peter Desaga, on an earlier design by Michael Faraday. The burner has a weighted base with a connector for a gas line and a vertical tube rising from it. There is a metal collar can be turned to close or partially close the air holes, thereby regulating the amount of air sucked in. The amount of air mixed with the gas stream affects the completeness of the combustion reaction in the flame (Jensen 2005). A special Bunsen burner with a flame separator called a "Smithells separator" invented by Teclu and independently by Smithells and Ingle more than 100 years ago (Smithells and Ingle 1892, Gaydon and Wolfhard 1970). In this burner, the outer diffusion flame is separated far from the inner rich premixed flame; therefore a very simple two-staged laminar combustion can be realized. A methane–air Smithells flame has been studied experimentally and numerically to investigate NOx reduction mechanism in methane–air Smithells flames (Nishioka et al. 2006). It has been found experimentally that the Smithells flames have about 40% less total NOx emission than Bunsen flames.

Flame stability is another topic investigated in the researches about combustion analysis. Stability limits of Bunsen flames have been investigated the influence of burner diameter on the blow-off limits of shielded and unshielded laminar flames. It is found that the limit of any given fuel-air mixture is independent of burner diameter in case of expressing as critical velocity gradient (Kurz 1957). In the study, the stability in the laminar diffusion flames of methane burned on small tubes have been investigated

and compared with the premixed methane-air flames (Robson and Wilson 1969). Flow velocity, temperature and composition have been measured over a small region near the flame base and it is found that near lift, the oxygen flux and gas velocity at the flame base in diffusion flames were similar to the values in premixed methane-air flames burning at the same temperature.

Flashback, which is a flame instability situation, is investigated for different conditions in various studies. The flashback gradients in the turbulent and laminar regions have been compared by Fine (Fine 1958). In this study, the effect of reduced pressure on the critical boundary velocity gradient for flashback has been investigated for laminar and turbulent burner flames. The comparison suggests that a turbulent burner flame near flashback is stabilized in the laminar sublayer. Flashback has been studied in the laminar premixed systems also numerically (Lee and T'ien 1982, Lammers and de Goey 2003). Lee and T'ien have examined flashback as a function of incoming velocity profiles, wall velocity gradients, and tube radius, and discussed the limitation of using the quasi-one-dimensional velocity balance concept as a predicting tool for flashback. Premixed flames, which are sensitive to flash-back in high-temperature combustion systems, has been studied numerically for methane/air combustion by Lammers and de Goey. It has been shown that stabilization on top of the foam is impossible for a range of velocities if the radiation temperature of the environment becomes too large and stabilization plots are presented from which the flash-back regions can be determined.

Emissions and flame stability have been investigated numerically for the lamella burner (Parmentier et al. 2001, 2003). In this study, 2D burner simulations have been performed with the object-oriented C++ code Gascoigne (Becker and Braack 2001) using detailed reaction scheme and transport model. It has been shown that flame temperature and toxic emissions increases when inflow velocity increases and the ambient temperature has a small and complex influence on the emissions. On the flame stability side, it has been found that the flame is exclusively stabilized through the long lamellae of the burner for an air equivalence ratio equal to or greater than 1.30.

In the optimization of the lamella burner fin deck, four alternative fin deck samples were produced and tested with current fin deck. After the evaluation of the test results, optimized design was defined, and the effect of the fin deck geometry on flame stability was focused on by investigating numerically unburned methane fractions,

which is one of the causes of carbon monoxide formation in exhaust. 2D combustion simulations were performed for two different geometries, which belong to the fin deck samples with different measured CO values, using Fluent 6.0 for an inlet flow velocity 0.2 m/s and an air equivalence ratio 1.20.

CHAPTER 3

LAMELLA BURNER FIN DECK LAYOUT

Fin deck layout parameters are determined analyzing the physical conditions and the combustion characteristics for fin deck. Pressure drop in the fin deck and surrounding temperatures influenced on the fin temperature are related with physical conditions for fin deck, and their effects on the combustion process will be investigated. Flame velocity (as a function of some physical and chemical properties), quenching, flame stabilization and flammability limits will be explained as being main characteristics of combustion. At the end of this chapter, layout parameters of the lamella burner fin deck will be determined using these analyses.

3.1. Integration of the Fin Deck

Lamella burner fin deck is connected to the lamella burner mixing chamber mechanically. The quick release fasteners are used for this connection (Figure 1.12). Fin deck is also integrated into the hydraulic system of the appliance in order to provide cooling water. Hydraulic integration is a must, since the fins have to be cooled continuously. Water cooling prevents destruction of the fin deck, increasing of the flame temperature and NOx formation rate.

In the 18 and 24 kW appliances, cooling water is realized by a hydraulic bypass from the central heating (CH) water (Figure 3.1). Hydraulic bypass allows ca. 40% of the CH water into the fin deck cooling pipe. If there is a serial flow through the fin deck, pressure drop occurs in the cooling pipe because of high flow rates of CH water.

In the 11 kW appliances, the CH water flows firstly trough the fin deck and then trough the heat exchanger (Figure 3.2). There is no pressure drop problem in the cooling pipes, since the flow rate of CH water is significantly lower than the 18 and 24 kW appliances.

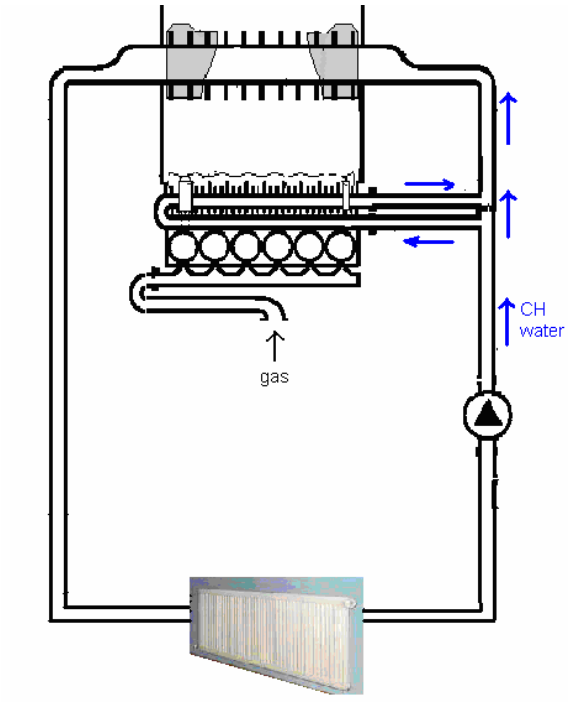

Figure 3.1. Hydraulic integration of the LBR fin deck into the 18 kW and 24 kW appliances (Source: Plothe and Sönmezışık 2003).

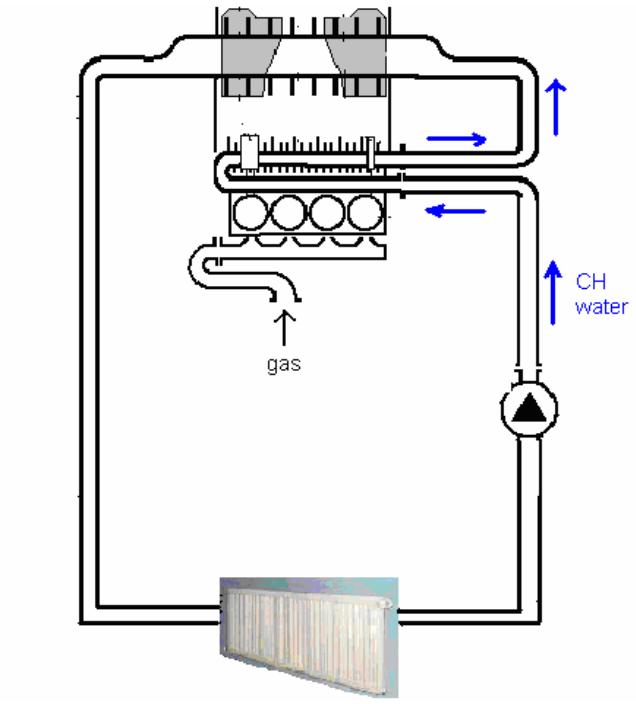

Figure 3.2. Hydraulic integration of the LBR fin deck into the 11 kW appliance. (Source: Plothe and Sönmezışık 2003)

There are some openings between the appliance and the combustion chamber in order to prevent pulsation. Secondary air comes into the combustion chamber but can not be included in the combustion process. Therefore it can be assumed there is no secondary aeration into the flames of the lamella burner.

3.2. Physical Conditions for the Fin Deck

Fin deck is an important part of the lamella burner, since combustion occurs on its surface. The fin deck is formed from several parts which influence combustion characteristics of the lamella burner. The physical conditions, which influence the combustion process, are pressure drop and temperature.

3.2.1. Pressure Drop in Fin Deck

Pressure drop in fin deck affects the burner combustion process mainly by influencing the primary aeration ratio of the burner. Primary aeration ratio, λ is one of the most important characteristics for combustion in fully premixed burner. Primary aeration in atmospheric burners (Figure 1.6) was explained in part 1.3.2, and the primary aeration ratio equation is defined as:

$$\lambda = \frac{1}{(x+\frac{y}{4})4.76}\left(\frac{d_M}{d_0} K \sqrt{\frac{\rho_g}{\rho_a}\frac{T_{amb}}{T_m}} - 1\right) \qquad (3.1)$$

It has not been mentioned in details about the K term, which refers to the mixing duct/burner coefficient. This term is inversely proportional to the burner/mixing duct resistance against the gas jet and air flow. This means, if the flow resistance of burner/mixing duct increase, the primary aeration ratio decrease, and vice versa. For mixing duct coefficient, shape and length of the mixing duct are the main influences on the flow resistance. As for burner coefficient, flow resistance is directly related to the physical blockage against the gas/air mixture (Figure 3.3).

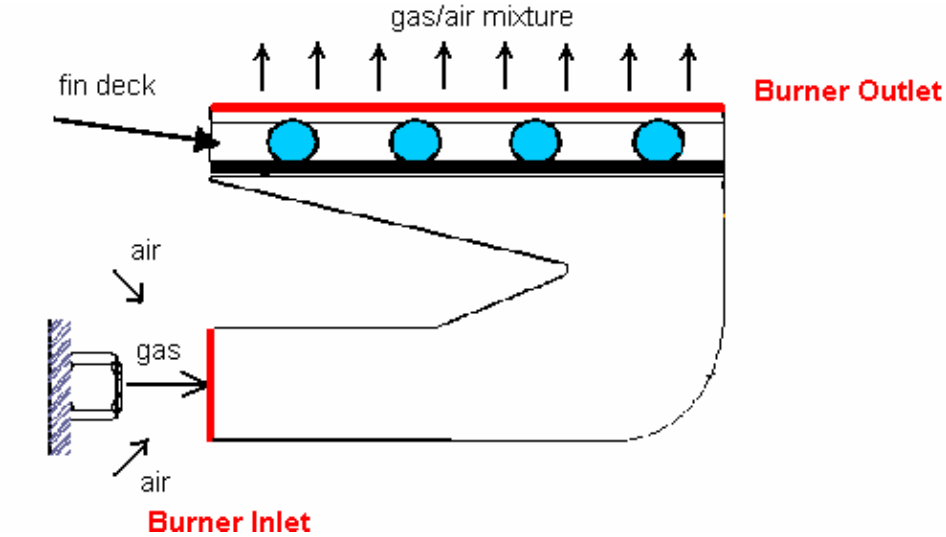

Figure 3.3. Burner inlet and outlet locations.

Fin deck is a resistance against the gas/air mixture flow coming from the mixing chamber. Flow resistance is determined as the ratio of pressure drop across an aperture to flow rate. Namely, flow resistance is proportional to pressure drop, and mass flow rate is inversely proportional to flow resistance and also pressure drop.

Pressure drop in fin deck can be defined by investigating the mass balance over the fin deck. There should be defined a control volume which shows fin deck inlet and outlet regions clearly (Figure 3.4). Hence the control volume includes some regions of mixing chamber and combustion chamber.

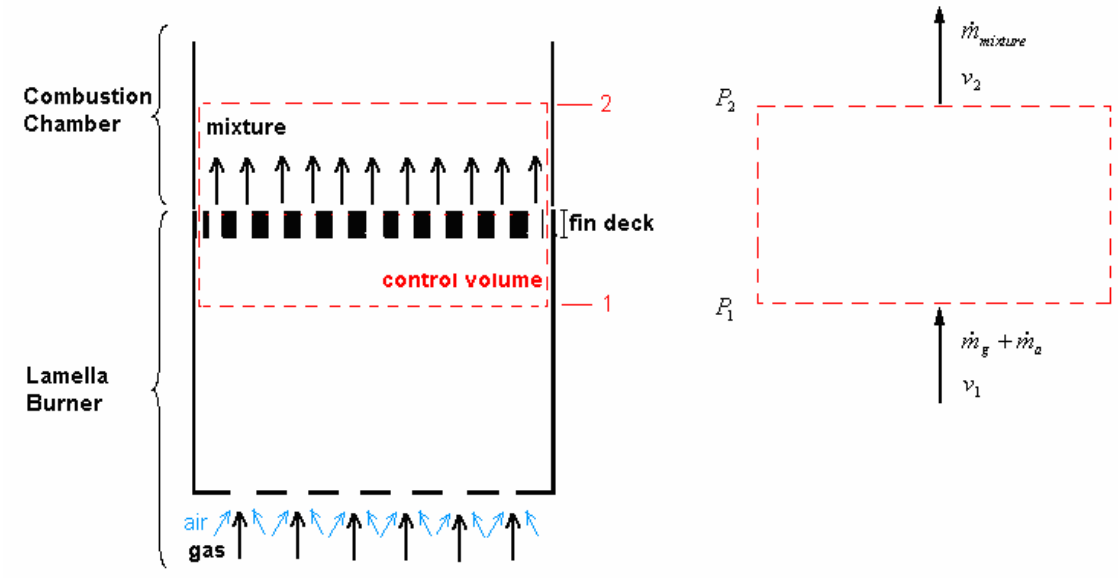

Figure 3.4. Control volume diagram for the fin deck.

If mixing chamber, fin deck and combustion chamber are assumed as a single body and any flow inlet/outlet through each connection are therefore neglected, conservation of mass can be used to investigate the mass flow rate of mixture in control volume. Therefore, the inlet and outlet mass flow rates are equal to each other. In the burner inlet, gas is injected by nozzles into the burner, and gas jet makes air also enter the burner. Therefore, mass flow rates of gas and air constitute inlet mass flow rate.

$$\dot{m}_{inlet} = \dot{m}_{outlet} \tag{3.2}$$

$$\rho_1 v_1 A_1 = \rho_2 v_2 A_2 \tag{3.3}$$

The inlet and outlet velocities are also equal because $\rho_1 = \rho_2$ and $A_1 = A_2$

$$v_1 = v_2 \tag{3.4}$$

Using Bernoulli equation (3.5), the pressure drop in the fin deck can be investigated.

$$P_1 + \frac{1}{2}\rho v_1^2 + \rho g h_1 = P_2 + \frac{1}{2}\rho v_2^2 + \rho g h_2 + \xi \tag{3.5}$$

where ξ is the losses in the fin deck. If the difference between h_1 and h_2 is neglected, it becomes as the equation (3.6).

$$P_1 + \frac{1}{2}\rho v_1^2 = P_2 + \frac{1}{2}\rho v_2^2 + \xi \tag{3.6}$$

Since $v_1 = v_2$, it can be written the equation (3.7).

$$P_1 = P_2 + \xi \tag{3.7}$$

Therefore;

$$P_1 > P_2 \qquad \text{and} \qquad \Delta P = \xi \tag{3.8}$$

Mass flow rate of the lamella burner is always related to the fin deck design. The outlet area of the burner is defined as the open surface of the fin deck, where the gas/air mixture passes through. Open surface is related to the number of fins, fin thickness and cooling pipe diameter. It can be easily calculated subtracting the total fin tip areas and the total cooling pipe diameters from the fin deck area.

The mass flow rate of gas/air mixture at the burner outlet is directly proportional to fin deck open surface. Since the mass flow rate of gas is fixed for a given output, any changes of the outlet mass flow rate influence only the mass flow rate of air inlet. The outlet mass flow rate only depends on the pressure drop in the fin deck. Therefore, the mass flow rate of air inlet is directly proportional to the open surface of the fin deck.

Since the flow resistance is inversely proportional to the burner coefficient, K in the primary aeration ratio equation, this resistance area of fin deck is also reversely proportional to K value. Open surface area of the fin deck is directly proportional to the K value in equation (3.1), and therefore decreases the flow resistance.

Briefly, pressure drop is one of the layout parameter related with open surface of the fin deck, since it influences the amount of the primary air inlet in to the burner.

3.2.2. Temperature Conditions

Temperature is another physical condition for the fin deck. There are three temperatures which influence fin temperature: flame, gas/air mixture and cooling water temperatures.

3.2.2.1. Effect of Flame Temperature

The temperature profile through the flame is an important characteristic of the combustion process and related with the type of the flame. Flames are categorized as being premixed flames and non-premixed flames according to their combustion types. Both premixed and non-premixed flames are also divided into two categories as being laminar and turbulent premixed flames according to their flow characteristics. Flames over the lamella burner fin deck are laminar premixed flames, since the combustion type of the lamella burner is fully premixed combustion and flames show laminar flow characteristics.

Flame structure can be investigated dividing the flame into two zones: preheat zone and reaction zone. In the preheat zone, there is released little heat; in the reaction zone, chemical enthalpy is converted into sensible energy. The temperature profile through the laminar premixed flame is illustrated in Figure 3.5 with other essential flame features.

If a combustion process takes places adiabatically and there is no work or changes in kinetic or potential energy during the process, the temperature of the product is referred to as **adiabatic flame temperature**. When the process occurs as a complete combustion without dissociation, the adiabatic flame temperature is the maximum temperature that can be achieved for the given reactants.

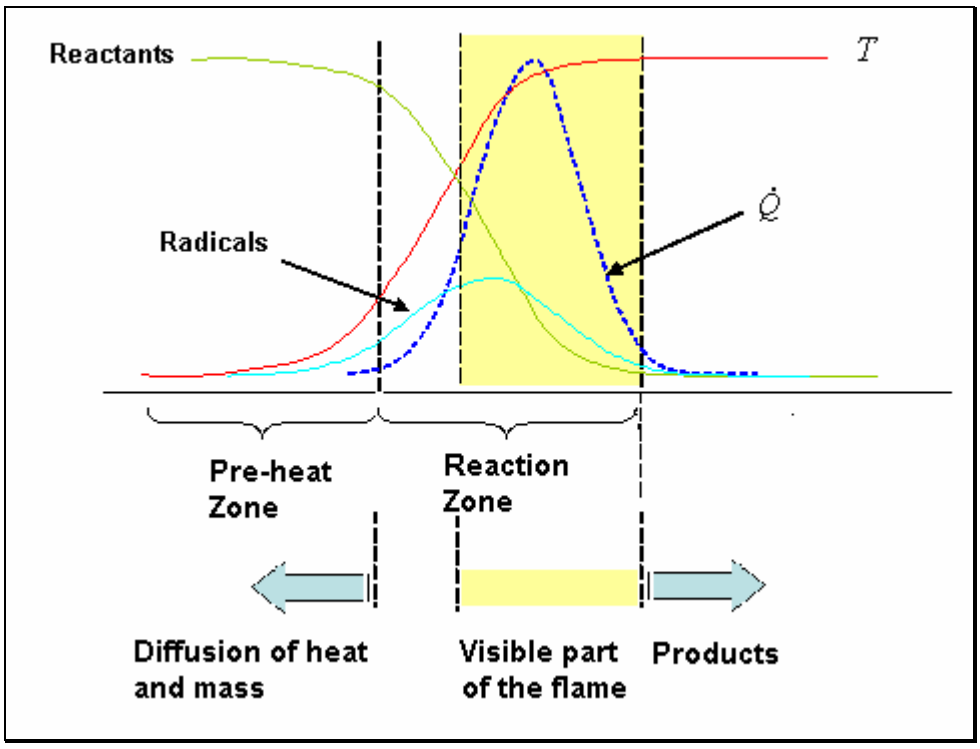

Figure 3.5. Laminar flame structure.

(Source: WEB_4 2003)

Two different adiabatic flame temperatures are defined: one for constant-pressure and one for constant-volume combustion. Burner combustion would be defined as constant-pressure combustion. If burner combustion process is assumed as an adiabatic process, the absolute enthalpy of the reactants at the initial state (T_i, P) equals the absolute enthalpy of the products at the final step (T_{ad}, P).

$$H_{reac}(T_i, P) = H_{prod}(T_{ad}, P) \tag{3.9}$$

Constant-pressure adiabatic flame temperature can be estimated for the combustion of the stoichiometric CH_4-air mixture (T_i =298 K, P =1 atm) using the following assumptions.

- Complete combustion process (no dissociation)

$$CH_4 + 2\,(O_2 + 3.76\,N_2) \longrightarrow CO_2 + 2\,H_2O + 7.52\,N_2 \tag{3.10}$$

- An initial guess for the adiabatic temperature, T_{ad}, should be made.

  For the products at the final step, an average of initial and final temperatures, $[(T_i + T_{ad})/2)]$, should be defined.

$$H_{reac}(T_i, P) = H_{prod}(T_{ad}, P) \tag{3.11}$$

$$\sum_{react} n_i h_i = \sum_{prod} n_i h_i \tag{3.12}$$

$$\begin{aligned}(n\,h^o_{f,i})_{CH_4} + (n\,h^o_{f,i})_{O_2} + (n\,h^o_{f,i})_{N_2} = {} & n_{CO_2}\left((h^o_{f,i} + c^o_{p,i}(T_{ad} - T_i)\right)_{CO_2} \\ & + n_{H_2O}\left((h^o_{f,i} + c^o_{p,i}(T_{ad} - T_i)\right)_{H_2O} \\ & + n_{N_2}\left((h^o_{f,i} + c^o_{p,i}(T_{ad} - T_i)\right)_{N_2}\end{aligned} \tag{3.13}$$

Where, T_i = 298 K, $h^o_{f,i}$ at 298 K, $c^o_{p,i}$ at $(T_i + T_{ad})/2$ =1200 K, since T_{ad} is guessed to be about 2100 K. Finally, T_{ad} = 2318 K after the iteration (Turns 2000).

The above method of calculation can be used sufficiently for flame temperatures below 1200 K. Since dissociation and formation of many other compounds occur at higher temperatures, the first assumption becomes invalid and the above method can not be used to find the exact adiabatic flame temperature. But it can give opinion for a rough estimation of the maximum flame temperature (Turns 2000).

3.2.2.2. Effect of Gas/Air Mixture Temperature

Fin deck is in direct contact with the gas/air mixture flow coming from mixing chamber, and fin temperature is therefore influenced from the mixture temperature by the way of convection between fins and mixture flow. It seems as if the gas/air mixture temperature influences the flame temperature, the change of flame temperature caused by preheating the initial mixture is not significant. The fact of that is clearly seen in the following equation (3.14) mentioned in the comprehensive theory of Zel'dovich, Frank-Kamenetsky, and Semenov, which is one of the laminar flame theories (Zel'dovich et al. 1938).

$$c_p T_0 + \frac{a_0 Q}{\rho_0} = c_p T_f \tag{3.14}$$

where, a_0 represents number of molecules of reactant per unit volume. Since the heat release term $\left(\frac{a_0 Q}{\rho_0}\right)$ is much larger than the term of thermal energy $\left(c_p T_0\right)$, T_f can not change much by the gas/air mixture temperature (Kuo 1986). In Figure 3.6, it is also showed that the change of flame temperature for different gas/air temperatures is very little (Parmantier et al. 2001).

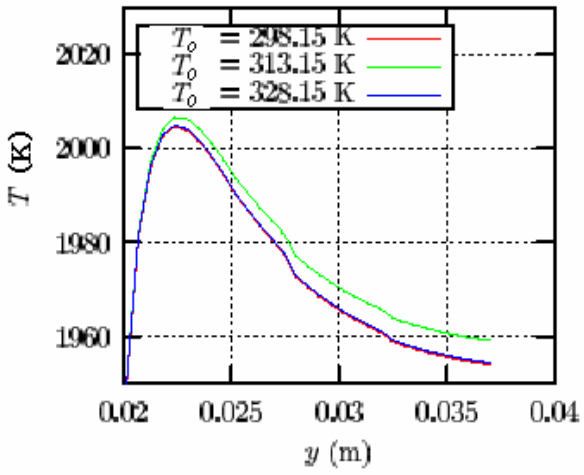

Figure 3.6. Flame temperature distribution with various mixture temperatures.

(Source: Parmantier 2001)

3.2.2.3. Effect of Cooling Water Temperature

Fins are continuously cooled during every operation of the appliance. Water cooling is a must to prevent deformation of fin deck and provide flame stability which will be discussed at the end of this chapter. For a low NO_x burner, cooling the fins is the main reason to reduce the thermal NO formation. Cooling water temperature depends on the flow rate of central heating water and the burner heat output. In a fin deck, cooling water is provided from central heating water. Before the flow becomes steady state, water flow rate influences the heat transfer rate from fins to cooling pipes and therefore cooling water temperature. Steady state conditions are related to the load of the appliance. After achieving the steady state condition, the inlet and outlet flow temperatures becomes constant and will not change relating to the flow rate. These constant cooling water temperatures are related to the burner heat output. They are at their highest values in maximum heat output of the burner and at their minimum values in minimum heat output.

3.3. Flame Velocity

In case of assuming that a flame is one dimensional and that the unburned gas/air mixture enters the flame in a normal direction, flame velocity S_L equals to the velocity of the normal component of unburned gas (relative to the flame front in opposite direction). A laminar premixed flame front ($\lambda \geq 1$) is illustrated as Figure 3.7 using the conical character of the flame, and there is shown the flame velocity vector.

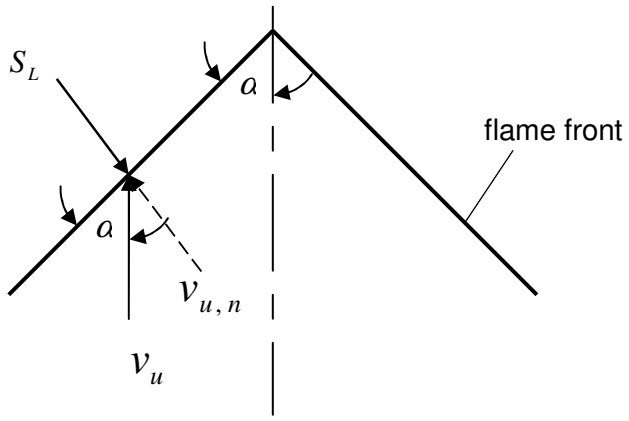

Figure 3.7. Laminar premixed flame front and laminar flame velocity.

(Source: Turns 2000)

Thus, the laminar flame velocity can be defined as:

$$S_L = v_u \sin \alpha \tag{3.15}$$

Flame velocity can be defined as a function of some physical and chemical variables in combustion process. Physical variables are temperature and pressure; chemical variables are primary aeration ratio and fuel type.

3.3.1. Influence of Temperature on Flame Velocity

Laminar flame depends strongly on temperature. Effect of gas/air mixture temperature on S_L can be clearly seen in Figure 3.8, which shows the experiment results of Dugger, Weast and Heimel for three different mixtures (Dugger et al. 1955).

The results can be represented by the relationship between flame velocity and mixture temperature as being $S_L \propto T_0^m$, where m ranges between 1.5 and 2.

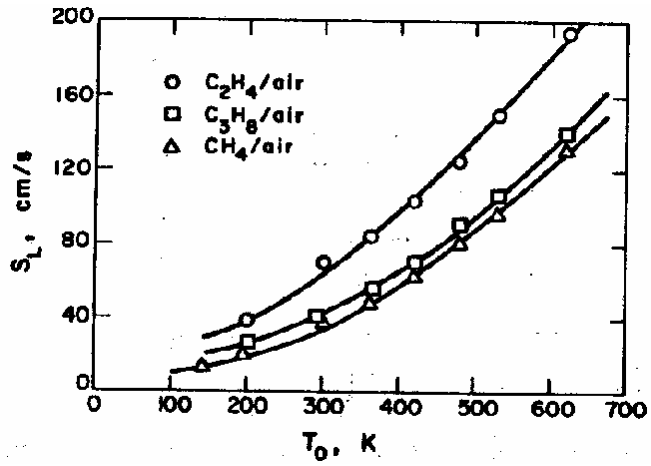

Figure 3.8. Effect of mixture temperature on flame speed.
(Source: Kuo 1986)

Flame temperature is another strong effect on laminar flame velocity. The maximum flame velocity for several mixtures is shown in Figure 3.9. At high flame temperatures, dissociations occur in the flame. Therefore, some free radicals produced and introduced into the flame. The lighter ones of the free radicals, like H atoms, are easily able to diffuse downward in the flame and can significantly enhance the flame velocity.

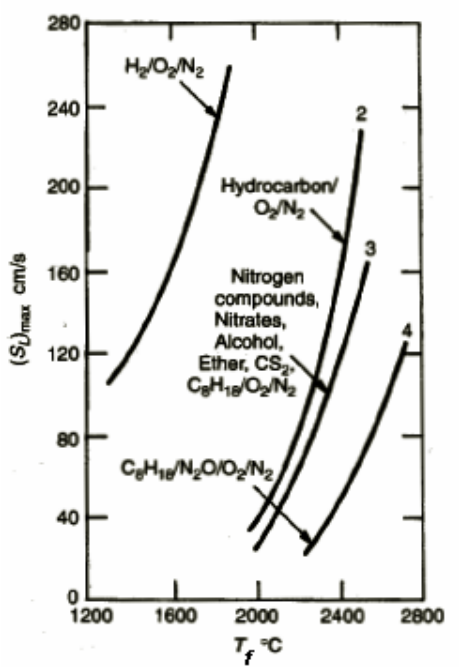

Figure 3.9. Effect of flame temperature on $(S_L)_{\max}$.

(Source: Kuo 1986)

3.3.2. Influence of Pressure on Flame Velocity

The effect of pressure on the laminar flame speed was studied, and a power law $(S_L \propto P^n)$ was developed by Lewis. The exponent n is referred to the Lewis pressure index. Laminar flame theories transform this equation to $S_L \propto P^{(n-2)/2}$, where the exponent n is the overall reaction order (Kuo 1986).

Overall reaction order is the sum of the reaction orders in the empirical formulation of the reaction rate. Definitions in an empirical formulation are shown in Table 3.1.

Table 3.1. Rate law (empirical formulation of the reaction rate)

Chemical Reaction	A + B $\rightarrow$ D + E
Empirical Formulation	$d[A]/dt = -k \cdot [A]^a \cdot [B]^b$
	$d[B]/dt = \ldots$
Rate Coefficient	k
Reaction Orders	a, b
Overall Reaction Order	a + b

For example, oxidation of methane is described as:

$$CH_4 + 2\ O_2 \rightarrow CO_2 + 2\ H_2O \tag{3.16}$$

The reaction rate with respect to CH_4 is described as following equation (3.17) taking H_2O into account, since water is not produced by a single collision of CH_4 and O_2 in reality (WEB_4, 2003).

$$d[CH_4] / dt = - k \cdot [CH_4]^{-0.3} \cdot [O_2]^{1.3} \cdot [H_2O]^{-0.7} \tag{3.17}$$

The overall reaction order of methane oxidation is found as:

$$n_{CH_4} = - 0.3 + 1.3 - 0.7 = 0.3 \tag{3.18}$$

Therefore, it is found that the pressure effect on the laminar flame velocity in CH_4 combustion as $S_L \propto P^{-0.85}$, which means laminar flame velocity in CH_4 combustion is influenced by pressure negatively.

3.3.3. Influence of Primary Aeration Ratio, λ on the Flame Velocity

Except very lean and very reach mixtures, effect of primary air ratio on the laminar flame velocity is similar to the effect of this parameter on flame temperature. The maximum flame velocity is observed in stochiometric or slightly fuel rich mixtures, and therefore it can be said a mixture with maximum flame temperature is the mixture with maximum flame speed (Kanury 1975). The behavior of CH_4 with respect to equivalence ratio ($1/\lambda$) and its percentage in mixture is shown in Figure 3.10.

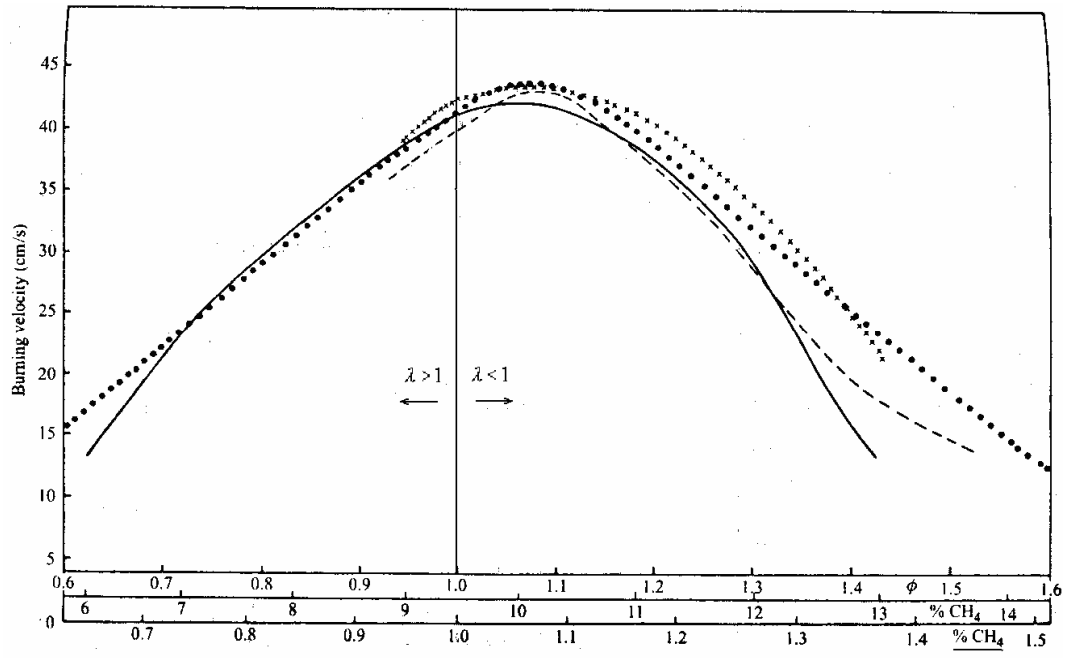

Figure 3.10. Effect of λ on the flame velocity of CH_4 (1 atm).

(Source: Turns 2000)

3.3.4. Influence of Fuel Type on Flame Velocity

The maximum flame velocity as a function of fuel type can be obtained it as a function of the number of carbon atoms in the fuel molecule for Alkynes (C_nH_{2n-2}), Alkenes (C_nH_{2n}), Alkanes (C_nH_{2n+2}) (Figure 3.11). Thermal diffusivity, which is a function of the fuel molecular weight, mainly causes the difference of S_L for fuels containing different numbers of carbon atoms (Kuo 1986). Some experimental data (Table 3.2) are also verifying Figure 3.11.

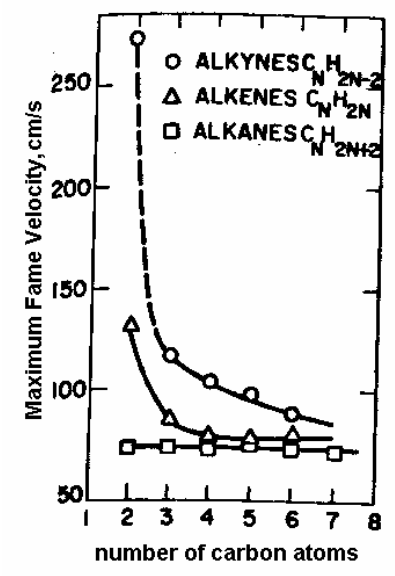

Figure 3.11. Effect of number of carbon atoms on $(S_L)_{max}$.

(Source: Kuo 1986)

Table 3.2. Laminar flame velocities for various pure fuels burning at 1 atm, λ=1, $T_{mixture}$=25˚C (Source: Turns 2000).

Fuel Type	Laminar Flame Velocity S_L, (cm/s)
CH_4	40
C_2H_2	136
C_2H_4	67
C_2H_6	43
C_3H_8	44
H_2	210

3.4. Quenching

For gas combustion in burners, it is clear that flames are forming on the combustion surface, which locates just after the burner outlet. Combustion surface does not propagate into the burner, since flames extinguish upon entering a small aperture. The critical diameter of the aperture, where flame can not propagate through, is defined as quenching distance (Tecce et al. 2005).

Quenching of the flames, which just enter through two parallel plates, is based on the energy balance between the rate of heat produced by chemical reaction and the rate of heat loss by conduction to the walls (Figure 3.12).

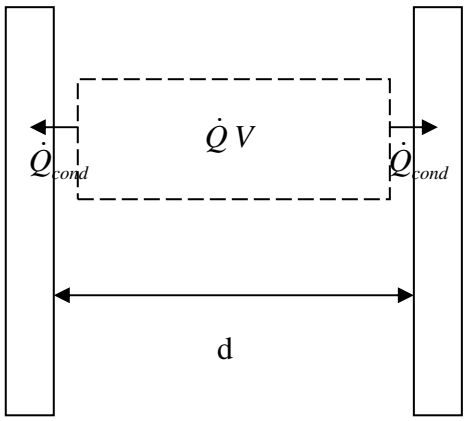

Figure 3.12. Flame quenching between two parallel walls
(Source: Turns 2000)

On the lamella burner fin deck, flames continually enter different apertures (Figure 3.13). First aperture is formed by two high fins; in the same way, second is formed by two low fins. High fins have cooling effect on flames significantly. But this effect does not mean quenching, since the distance between high fins (4.5 mm) is too large to extinguish the flame. Cooling effect of high fins only narrows the flame diameter. After its diameter becomes narrower, flame enters the apertures formed by low and high fins. In this case, flames are quenched, since the distance between all fins (1.5 mm) is smaller than the limit quenching distance for most hydrocarbons. Briefly, quenching occurs between all the fins of the fin deck, since the distances between the fins satisfy flame quenching.

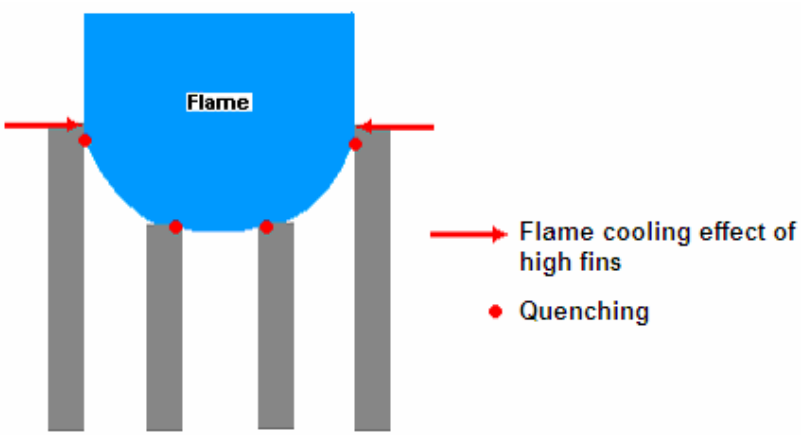

Figure 3.13. Flame cooling of high fins (between the red arrows) and quenching (between the red points) on the lamella burner fin deck.

3.5. Flame Stabilization

Flame stabilization is an important design criterion for gas burners and related to gas/air mixture and laminar flame velocities. The comparison of mixture velocity and the laminar flame velocity profiles near the rim (fin edge for the LBR fin deck) shows clearly the critical conditions for lightback and liftoff (Fig. 3.14).

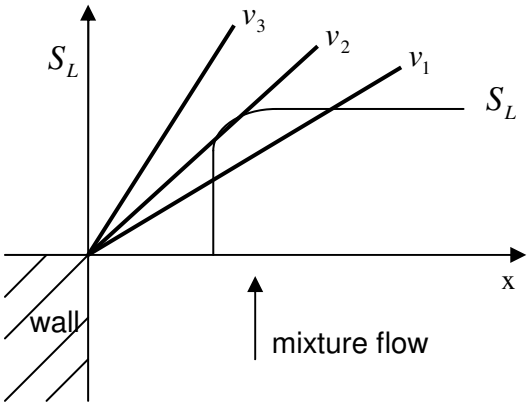

Figure 3.14. Flame and mixture velocity profiles of a laminar premixed flame. (Source: Cerbe 1986)

When the mixture flow rate is very low, the flame velocity is greater than the mixture velocity (v_1), hence the flame propagates through the burner and lightback occurs. It is known that premixed flames are sensitive to lightback through the apertures in high temperature combustion systems, which are investigated in a numerical study of flash back of laminar premixed flames in ceramic-foam surface burners (Lammers and de Goey 2003) When the mixture velocity (v_2) and flame velocity are equal, flame is stable. When the mixture flow rate is very high, the mixture velocity (v_3) is greater than the flame velocity. Then unburned gas/air mixture becomes diluted by diffusing of surrounding gases and flame lifts off. In combustions with high velocity mixture flows, lifted jet flames can be also stabilized. Flame stabilization mechanisms in axisymmetric jet flows are investigated by Chen and Bilger (2000) for lifted laminar propane flames.

There should be finally mentioned about one more phenomena related to flame stability, which is yellow tipping and related to gas quantity in the gas /air mixture. Schalla et al. have explained yellow tipping as: “When a premixed flame is made

increasingly richer, a point is reached at which a yellow tip appears on the flame. If the air supply is reduced still further, the yellow tip increases in size until the whole flame is luminous." (Schalla et al. 1954)

In Figure 3.15, there is shown the stability diagram for flash back, liftoff and yellow tipping for natural gas.

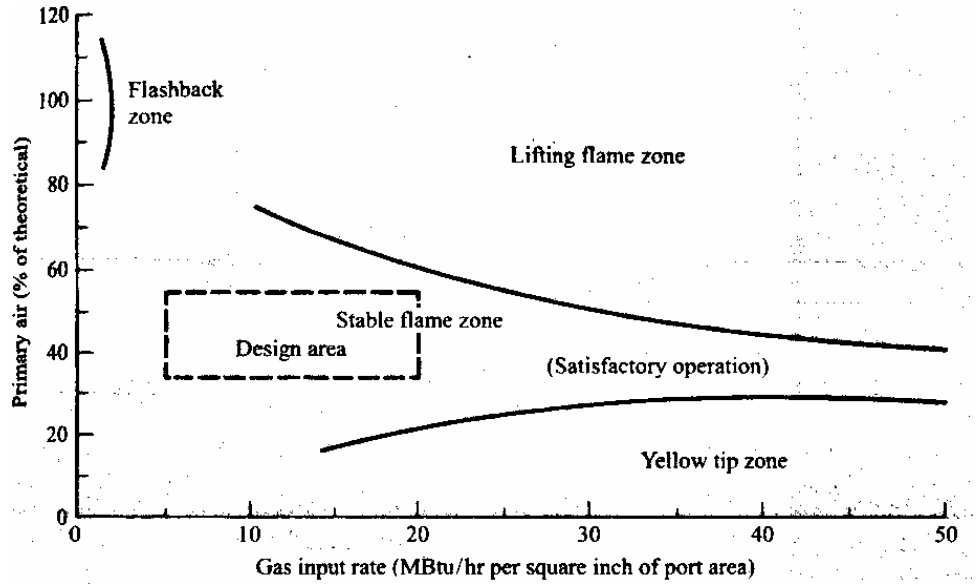

Figure 3.15. Flame stabilization for natural gas (for a burner with single row 2.7-mm-diameter and 6.35 mm spacing) (Source: Kuo 1986).

3.6. Flammability Limits

Flames propagate only between the lower and upper limits of flammability. Lower and upper flammability limits represent the leanest mixture ($\Phi < 1$) and the richest mixture ($\Phi > 1$) for steady flame propagation, respectively. They are also represented as the percentage fuel by volume in the mixture. Table 3.3 shows lower and upper flammability limits of some gas/air mixtures.

Pressure and temperature effect definitely on the flammability limits. The upper limits becomes much wider with increasing pressure, however the lower limits are not appreciable affected by pressure (Figure 3.16). However, the effect of temperature is less significant than the effect of pressure; the flammability limits are broadened with the increase of temperature. Experimental studies show that the limits vary linearly with temperature.

Table 3.3. Flammability limits and quenching distances for various fuels.

(Source: Turns 2000)

Fuel	Flammability Limits			Quenching Distance (mm)
	Lower Limit Φ_{min}	Upper Limit Φ_{max}	Stoichiometric Mass Air-Fuel Ratio	
H_2	0,14	2,54	34,5	0,61
CH_4	0,46	1,64	17,2	2
C_3H_8	0,51	2,83	15,6	1,8

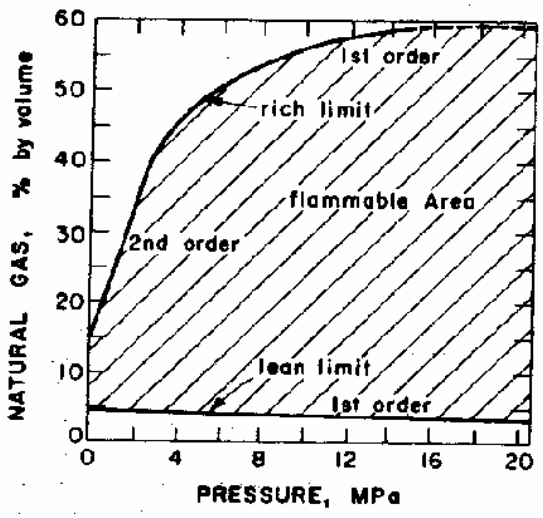

Figure 3.16. Effect of pressure on the lower and the upper flammability limits.

(Source: Kuo 1986)

3.7. Fin Deck Layout Parameters

Parameters, which affect the conditions mentioned in this chapter, can be used as the layout parameters of the lamella burner fin deck. In Table 3.4, the subtitles of this chapter and the parameters were listed in rows and in columns, respectively. The marked cells shows the parameters related with the subtitles.

Table 3.4. Fin deck layout parameters

COMBUSTION CONDITIONS	LAYOUT PARAMETERS								
	Open Surface	T_{FLAME}	$T_{MIXTURE}$	$T_{COOLING}$	T_{FIN}	λ	Fin to fin distance, d	Flame Velocity, S_L	Mixture Velocity, $v_{mixture}$
Pressure Drop in Fin Deck	X								
Temperature Conditions for Fin Deck		X	X	X					
Flame Velocity, S_L		X	X			X			
Quenching					X		X		
Flame Stability						X		X	X
Flammability Limits						X			

CHAPTER 4

LAMELLA BURNER FIN DECK DESIGN

4.1. Present Design of Fin Deck

In lamella burner, fin deck design is fairly important design, since fin deck is closely related with combustion and any lack in its design can be the cause of big problems. Fin deck consists of some different parts, and main parts of the fin deck are water cooled fins and frame.

4.1.1. Fin Design

In lamella burner, gas/air mixture flow through the fins and then flames occur on the combustion surface. In Chapter 3, combustion parameters are investigated and it is seen that flame stability is strongly related to the fin design.

Main function of the lamella burner fins is stabilizing the flames at the lowest pressure drop. Since fin temperature is most important parameter for flame stabilization, fins are continuously cooled by water during the combustion process. All of the fins are punched in order to provide passing four copper tubes through them (Figure 4.1).

Figure 4.1. Drawing of a punched low fin.

Number of cooling pipes was defined as four after the trials using number of pipes as being four and more and less than four. When more then four pipes were used, open surface of fin deck gets smaller and hence pressure drop increases. On the other hand, when less then four pipes were used, total cooling effect of water flow reduced and fins could not get cool enough. After deciding the number of pipes as four, the diameter of cooling pipes was defined as 13 mm, since it is the suitable to provide both lower hydraulic pressure drop in the water pipes and lower flow resistance against the gas/air mixture.

Fin heights were determined according to cooling pipe diameter in order to have enough space for punching operations of fins, especially low ones. Then, the height of high fin was defined as being 2 mm higher than low ones (Figure 4.2). As for fin thickness, it is 1 mm for all fins.

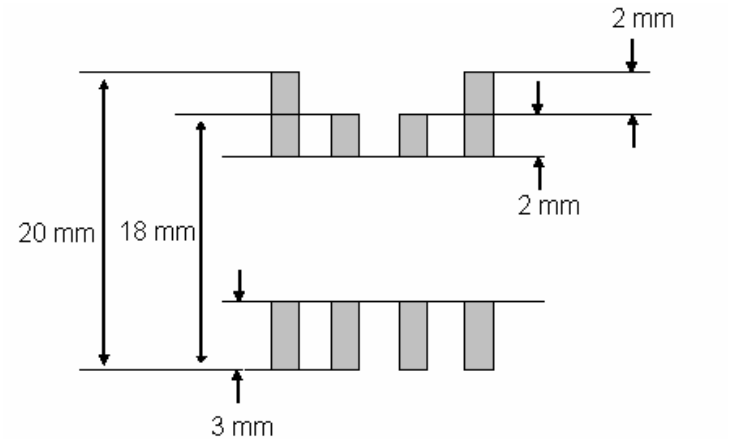

Figure 4.2. Dimensions of low and high fins.

The connection between fins and cooling pipes are provided after two processes. First, copper tubes are mechanically extended after passing them through the fins. Second, brazing process is applied. Therefore, fin and pipe materials are connected with a filler metal. Brazing process should be successful in order to provide heat transfer from fins to the water in the cooling pipes. Therefore, fins can be cooled continuously and quench the flames not exceeding the critical temperature during the operation. Light back is observed, when the fin deck without brazing is used in the operation.

Material is another important design parameter of the fins. Fin material must have good resistance to corrosion in exhaust gases and oxidation at high temperatures. %17 chromium ferritic stainless steel, which is intensive to stress corrosion cracking like all ferritic stainless steels and has good resistance to oxidation up to 980˚C, is used as the fin material of the lamella burner fin deck. Any other possible materials able to use as the fin material are under investigation.

Flame quenching is one of the main properties of combustion. Since combustion occurs on the fin deck surface, its design is closely related to quenching. In order to prevent flame propagation through the fins, and hence lightback, fin to fin distance is determined as 1.5 mm, which is derived from the quenching distance between two

parallel walls for a critical gas propane (Table 3.3). Propane is the most critical gas for light back in the using gasses for lamella burner, since its maximum flame velocity is higher than the especially methane (Table 3.2).

Quenching distance narrows with increasing gas/air mixture temperature, since flame is able to propagate through smaller apertures at high wall temperatures. In lamella burner fin deck, mixture temperature is strongly influenced from the fin temperatures. Therefore, it is very important to keep the fins at suitable temperatures. In order to satisfy flame quenching, fins are cooled with water continuously. Fins and cooling tubes are brazed in order to increase heat transfer rate from fins to cooling water. Unbrazed fins do not have enough touching area between fins and pipes, therefore fins can not be cooled enough and lightback occurs.

4.1.2. Frame Design

The other main part of the fin deck design is frame. Fins are surrounded by the frame; therefore fin deck has mechanical stability. Frame is formed from two U – profiles, two end fins and four collars. End fin is considered as the side part of the frame because of its design, which provides mechanical stability. 1mm-thick U - profiles are connected to the fins by welding and touch the end fins (Figure 4.3). Four collar parts are joined each other and placed on the end fins and the U – profiles mechanically (Figure 4.4).

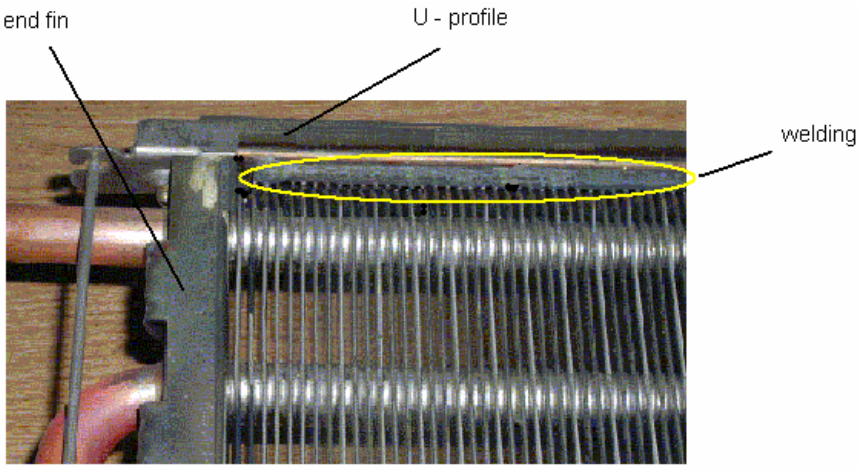

Figure 4.3. Connection of the U- profile to the fins (bottom view of fin deck).
(Source: Plothe and Sönmezışık 2003)

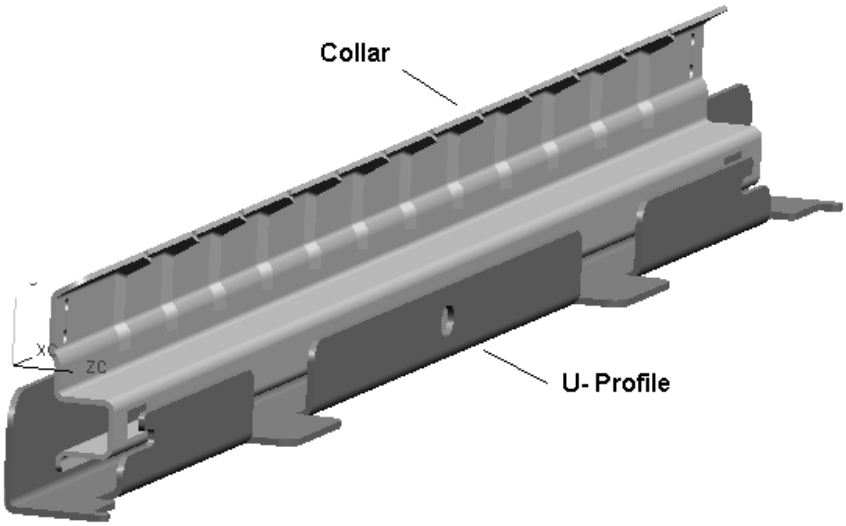

Figure 4.4. Frame parts (back side parts).

Frame temperature is an important design criterion for fin deck. Since frame is touching continuously to the sealing material, frame temperature should be less than 250°C. Otherwise, sealing material will destroy, hence gas leakage will occur. Two-part frame design and the welding process between fins and frames are therefore important in order to reduce frame temperature.

U – Profiles, which are welded to the fins, are connected to the mixing chamber with fasteners. U – Profile in front of the deck has cuts, where the fasteners hang on (Figure 4.5). Two pawls, which are welded on the back profile, is nailed together with mixing chamber and apply counter load to the fasteners. Therefore, lamella burner becomes a robust body from two separated parts.

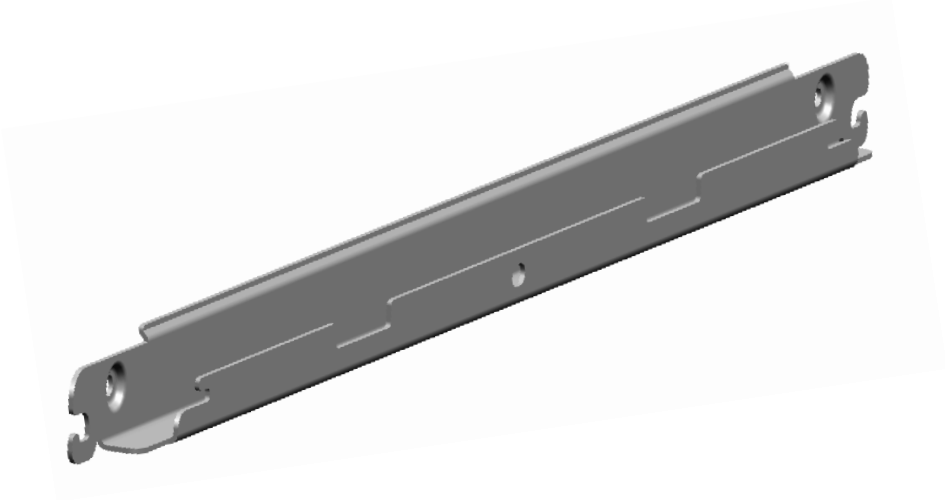

Figure 4.5. U – Profile (in front of the fin deck).

Profiles are produced from the fin material, in order to succeed the welding process between fins and profiles. It is also an advantage to use ferritic stainless steel material because of its high mechanical strength property.

There are used collars to prevent secondary air inlet into the combustion surface. In case of secondary aeration into the flame, flame gets cooler and incomplete combustion occurs. As it was mentioned about in Chapter 3, CO production is a result of partial combustion of the unburned hydrocarbon molecules in incomplete combustion processes. Therefore, increase in CO emissions is prevented using collars as barriers against the secondary air.

The small cuts on the collars are needed to provide the part against bending because of the thermal expansion (Figure 4.6). Without any cuts, there would be observed bending and crackling noise problems on collars. The cuts have to be certainly as small as possible in order to prevent secondary aeration into the combustion chamber. Therefore, cuts on the collars of lamella burner fin deck have to not exceed 1 mm. The steel group of collar material is heat resistant steels with >2.5% Ni. This material has high thermal strength and therefore suitable as collar material, which is face to face with radiation during the all combustion process.

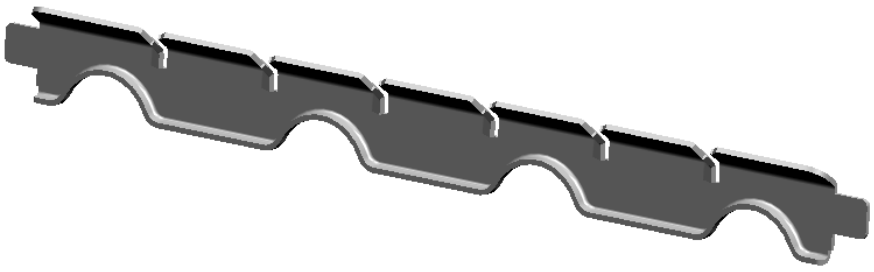

Figure 4.6. Collar (on the end fin).

4.2. Alternative Samples

There are totally four fin deck samples were designed for 24 kW appliances. These samples can be investigated under two main groups, which are different from current fin deck design with their fin thickness, are coded as 5004 and 5006 samples.

Main design change in 5004 and 5006 samples is the new fin thickness. Fin thickness in serial deck is 1mm, where it changes to 0.6 mm in 5004 and 5006 samples.

In addition fin sides are bended order to increase the touching surface between fins and frames. Since there are no differences in the dimensions of fin deck, the fin numbers and some physical properties of fin deck like its open surface are changed. The only difference between two samples is their fin heights. 5004 sample is formed from the fins, which are in the same heights. As for 5006 sample, it is formed from 1-high and two low-fins alike the original fin deck. 5004 and 5006 samples are therefore called as even deck and step deck, respectively.

Both 5004 and 5006 samples have two different versions. 5004-1 and 5004-2, 5006-1 and 5006-2 are the first and second versions of the 5004 and 5006 samples. The main difference is first versions (5004-1 and 5006-1) are produced without welding between fins and frame. In the second (5004-2 and 5006-2) versions, frames are welded to the fins. 5006-2 is different than the all of the other versions. It has not only the welding process and bended fins but also 0.6 mm thickness of frame material.

There are given the design parameters of original fin deck and samples in Table 4.1.

Table 4.1. Design parameters of the lamella burner fin deck.

	Design Parameters
Fin	Fin thickness (mm)
	Number of fins
	Fin heights (mm)
Frame	Frame design
	Frame thickness (mm)
	Frame temperature (°C), max
Cooling Pipe	Number of cooling pipes
	Cooling pipe diameter (mm)
Fin - Frame Connection	Welding

CHAPTER 5

LABORATORY TESTING

Lamella burner is used in two different combi boiler types. Burner tests are performed under different conditions for each combi boiler. Therefore, all of the standard tests for LBR are defined according to the combi boiler types.

5.1. Combi Boiler Types of LBR

Gas Fired Combination Boilers (so called "combi-boiler") are appliances that generate heat for two functions: central heating and domestic hot water production. Therefore, unlike a conventional system, a combination boiler does not store hot water. Instead it heats water directly from the cold mains. They are working with either natural gas or LPG.

The major components of a combi boiler are as followings.

- Gas valve
- Draught diverter / Flue hood with fan
- Burner
- Heat exchanger
- Pump
- Control system

Combi boilers can be classified according to the type of some components. Burner is one of these components. Combi boilers are divided into two as being conventional and low NOx boilers according to their burner types. They are also divided into two as being OF (open flue) and RSF (room sealed flue) boilers according to the mode of evacuation of the combustion products and admission of the combustion air.

Since lamella burner is a low NOx burner, the appliances containing lamella burner are low NOx appliances. These appliances using lamella burner have two types as being Room Sealed Flue (RSF) and Open Flue (OF) appliances (Figure 5.1, 5.2).

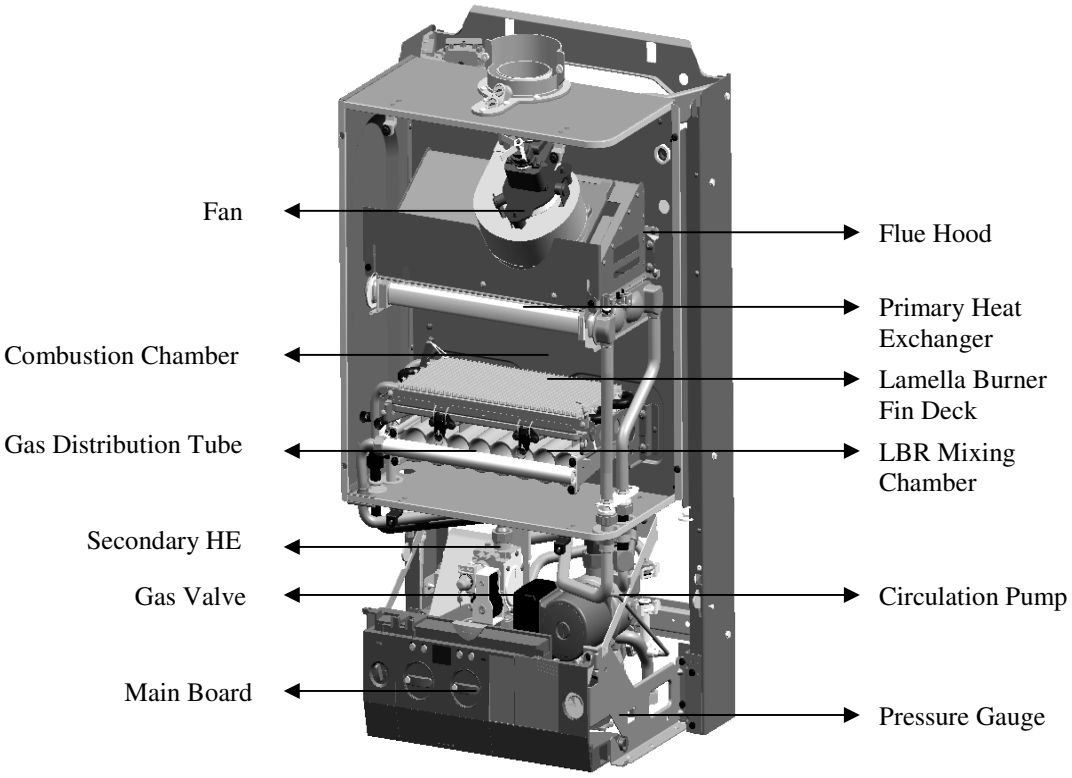

Figure 5.1. Model of RSF low NOx combi boiler (24 kW).

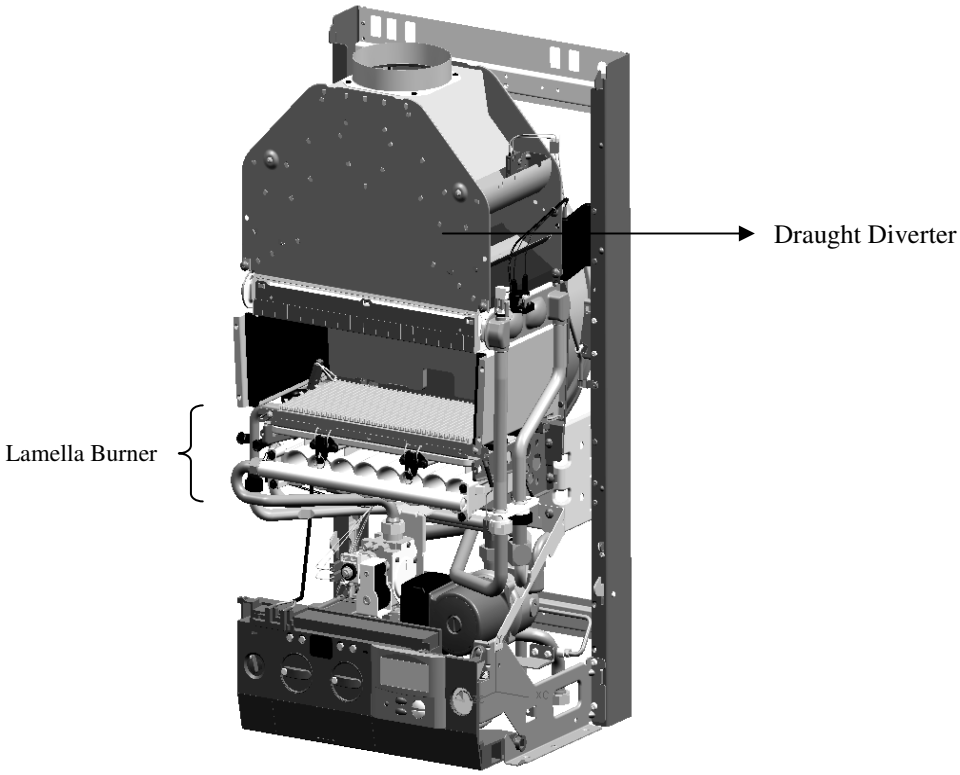

Figure 5.2. Model of OF low NOx combi boiler (24 kW).

5.2. Testing

Equal tests were performed for the current and new designs of lamella burner fin deck. These tests can be collected under two test groups as being standard tests and special tests. Standard tests include emission tests, light back test and flame lift test. Temperature and pressure tests were determined as special tests for fin deck designs.

5.2.1. Test Rig

Standard tests and temperature tests were performed on the test rig of Development Department in BOSCH, Manisa. The tests are performed for both OF and RSF appliances in this test rig. The appliance assembly part is available for all kind of appliances. Test rig is connected to the test gas, propane and LPG tubes, line gas and main water. The test appliance provides gas and water (domestic hot water, central heating water) from the test rig. In the test rig, there are some circuits such as domestic hot water, central heating water, cooling water circuits.

The test rig is software controlled. Flow rate, pressure and temperature data are read both on the electric panel of test rig by digital indicators and on PC.

The pressure drop test rig was designed and built for this project. This test rig was designed to measure the pressure drop in a LBR fin deck. The aim of this design is to fix the fin deck in a construction allowing the airflow pass through the deck only in one direction (Figure 5.3).

There are two venturis in the same distance before and behind of the fixed fin deck. Venturi is used for measuring pressure difference. They are connected with an Air - Pro to measure the difference between the pressures of two locations, which means the pressure drop in LBR fin deck. Since the pressure drop is related with the flow velocity, an anemometer is located just before the fin deck.

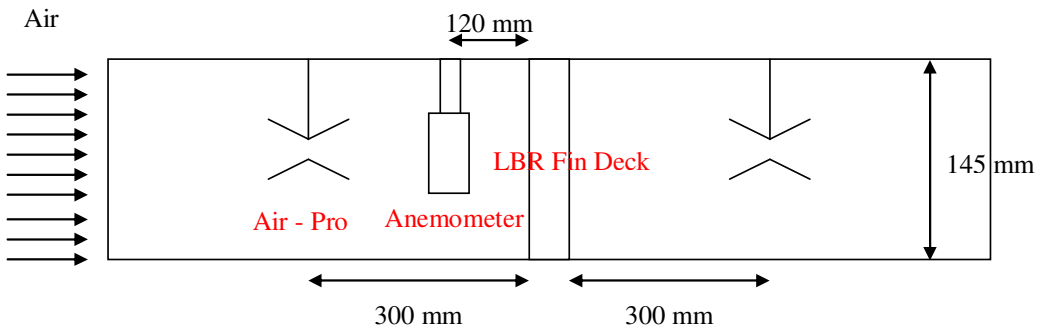

Figure 5.3. Pressure drop test rig.

5.2.2. Measurement Equipments

There are various measurement equipments used in this project. Some of them are the fixed equipments on the test rig in development department. Main properties of these equipments are shown in Table 5.1.

Table 5.1. Properties of measurement equipments in used test rig.

	Type	Brand	Range	Tolerance
Gas circuit				
Gas temp.	thermo couple		0-100℃	±0.05 K
Gasmeter pressure	SEN 3251-B146	SMS	0-250 mbar	%0.50
Burner inlet pressure		Siemens	0-50 mbar	%0.10
Gas pressure		Siemens	0-50 mbar	%0.11
DHW circuit				
Inlet water temp.	Pt-100	tetcis	0-100℃	%0.10
Outlet water temp.	Pt-100	tetcis	0-150℃	%0.10
DHW flow rate-electrical	MID	Siemens	0-15 l/min	%0.25
DHW flow rate-mechanical	Glass Tube	Rotameter	1.7-17 l/min	
CH circuit				
İnlet water temp.	Pt-100	tetcis	0-100℃	%0.10
Outlet water temp.	Pt-100	tetcis	0-150℃	%0.10
CH flow rate	MID	Siemens	0-26 l/min	%0.25
CH flow rate-mechanical	Plastic tube	Rotameter	3-30 l/min	
CH inlet pressure	SEN-3247 B065	Kobolt	0-6bar	%0.10
Cooling water circuit				
Inlet water temp.	Pt-100	tetcis	0-100℃	%0.10
Outlet water temp.	Pt-100	tetcis	0-150℃	%0.10
Cooling flow rate-mechanical	Plastic tube	Rotameter	3-30 l/min	
Ambient Data				
Ambient temperature per rig	Pt-100	tetcis	0-100℃	%0.10
Air humidity ratio (1 in room)	HC 322	rotronic	0-100 %rF	
Atmospheric pressure (1 in room)		Siemens	915-1113 hPa	%0.10
free thermocouples	thermo couple		0-100℃	±0.05 K
Data acquisition				
Field point (8) thermocouple module	FP-TC-120 Module			

For the emission tests, gas analyzers are used to measure the rates of combustion products in the exhaust gasses. In the laboratory, the S700 modular system analyzes the gas components. S700 housing is equipped with up to 3 analyzer modules. These analyzers monitor the level of NO and CO particles (ppm) and CO2 percentage (%). The technical specification of the used gas analyzer is shown in Table 5.2.

Table 5.2. Technical specification of the used gas analyzer

Brand	**SICK**MAIHAK
Type	Modular System S700
Measured components	NO, CO,CO2
Measurement principle	NDIR, thermal conductivity, interference filter correlation, rotating diamagnetic dumbbell, electrochemical cell
Measuring gas pressure	16 ... 250 hPA (0.23 ... 3.6 PSI)
Measuring gas temperature	0 ... 45 °C (32 ... 113 °F)

Thermocouples were used to measure the temperature of some points on the fin deck. They are connected to the test rig on the thermocouple modules. 8 different temperatures on the appliance, hence on the fin deck in this project, are measured in the same operation. The temperatures are recorded during the operation. The properties of the thermocouples are the same with the thermocouple properties in the Table 5.1.

In the pressure drop test rig, the pressure difference is measured with a flow meter. The other measurement equipment is used in that test rig is anemometer. Their technical properties of these instruments are shown in Table 5.3.

Table 5.3. Properties of flow meter and anemometer

Brand	AirPro	
Type	FCO520 Portable Flowmeter	Anemometer
Accuracy		±2%
Range	0 - 600 Pascals	0.4 - 30 m/s
Properties	Has averaging features and data entry for volume flow, mass flow and absolute pressure.	portable, provides fast and accurate reading with digital dispaly

5.3. Test Procedures

5.3.1. Standard Tests

Standard tests are performed according to EN standards, EN 297 and EN 483, which were defined for both RSF and OF appliances. The standard EN 297 was prepared for the gas-fired central heating OF boilers fitted with atmospheric burners of nominal heat input not exceeding 70 kW. The other standard EN 483 was prepared for the gas-fired central heating RSF boilers of nominal heat input not exceeding 70 kW.

In EN 297 and EN 483, there are standardized all of the requirements to produce combi boilers, which deal with aspects related to safety, rational use of energy and fitness for purpose. If the manufacturer indicates that the boiler has been tested in accordance with EN 297 or EN 483, the boiler must comply completely with the requirements of that standard. In spite of being performed all of the required tests in BOSCH Thermotechnologies, Manisa, in this study, the tests only related to the fin deck design are mentioned about.

During the tests, the test gases are used, which are defined in the EN standards. There are shown all of these gases for the appliances working with natural gas and LPG in Table 5.4 and Table 5.5, respectively.

Table 5.4. Test gases for the combi boilers working with natural gas.

(Source: The European Standard EN 297:1994 2003, The European Standard EN 483:2000 2002)

Reference Gas	G20	CH_4 = 100
Incomplate Combustion and Sooting Limit Gas	G21	CH_4 = 87 C_3H_8 = 13
Light Back Limit Gas	G222	CH_4 = 77 H_2 = 23
Flame Lift Limit Gas	G23	CH_4 = 92,5 N_2 = 7,5

Table 5.5. Test gases for the combi boilers working with LPG.

(Source: The European Standard EN 297:1994 2003, The European Standard EN 483:2000 2002)

Reference Gas, Incomplate Combustion and Sooting Limit Gas	G30	n-C_4H_{10} = 50 i-C_4H_{10} = 50
Flame Lift Limit Gas		C_3H_8 = 100
Light Back Limit Gas	G32	C_3H_6 = 100

5.3.1.1. Emission Tests

Two different tests are performed in order to determine the emission rates. One of them is done to determine the number of NO particles in exhausts according to the procedure of NOx test (MAN E001), and the other one is done to determine the number of CO particles according to the procedure of “Combustion Performance Curve” test (MAN E002).

In each test, the NO and CO values have to be determined for air free combustion products. AFNO and AFCO are the calculation methods of NO and CO values, which is defined in EN Standards for the stochiometric combustion processes. It is a must using AFNO and AFCO values to compare the emission levels of the

appliances under the same conditions. For both two tests, NO and CO values are also defined as being AFNO and AFCO values.

Air ratio in flue pipe, λ has to be defined to calculate AFNO and AFCO values. λ is defined by measuring CO_2 percentage in exhaust gases and choosing the nominal CO_2 percentage in Table 5.6 as being:

$$\lambda = \frac{(CO_2)_N}{(CO_2)_M} \tag{5.1}$$

Table 5.6. $(CO_2)_N$ concentration of combustion products, in percent.
(Source: The European Standard EN 297:1994 2003, The European Standard EN 483:2000 2002)

Designation of the gas	G 20	G 21	G 23	G 25	G 26	G 27	G 30	G31
$(CO_2)_N$	11,7	12,2	11,6	11,5	11,9	11,5	14	13,7
Designation of the gas	G 111	G 120	G 130	G 140	G 141	G 150	G 231	G 271
$(CO_2)_N$	7,6	8,35	13,7	7,8	7,9	11,7	11,5	11,2

Therefore, AFCO and AFNO values are calculated as followings.

$$AFNO = \lambda\,(NO)_M \tag{5.2}$$

$$AFCO = \lambda\,(CO)_M \tag{5.3}$$

"NOx Test Procedure" is defined below:

- A 300mm horizontal flue (+ restrictor if used) and 1000mm horizontal flue are used for RSF and OF appliances, respectively.
- The appliance must reach thermal equilibrium at each heat input before the NOx is measured. The NOx is measured at the heat inputs given in the Table 5.7.

Standards require that this test must be done with the required return temperature. If the minimum heat input is greater than 20% but less than 40% then NOx is measured at the minimum heat input and not at 20%. The Weighting Factor will be 0.30 in this case but the return temperature has to be calculated using the following formula;

$$\boldsymbol{T_r = 0.4Q + 20} \tag{5.4}$$

where $\boldsymbol{T_r}$ = return temp. °C

Q = measure heat input as a percentage

Table 5.7. Heat inputs for NOx test.

(Source: The European Standard EN 297:1994 2003, The European Standard EN 483:2000 2002)

Heat Input	Return Temperature	Flow Temperature	Weighting Factor
	60°C	80°C	0
70%	48°C	Note	0,15
60%	44°C	Note	0,25
40%	36°C	Note	0,30
20%	28°C	Note	0,30

• The measured NO values are converted to the AFNO values. After that, these values are evaluated in mg/kWh, and NOx classes are defined (Table 5.8).

Table 5.8. NOx classes.

(Source: The European Standard EN 297:1994 2003, The European Standard EN 483:2000 2002)

NO_x Classes	**Limit NO_x concentration in mg/kWh**
1	260
2	200
3	150
4	100
5	70

This procedure is only valid for modulating appliance which will use second family gases.

"Combustion Curve Test Procedure" is defined below:

• The restrictive flue (for each flue type) and 1000mm flue are used for RSF and OF appliances, respectively.

• The appliance must be operated at minimum heat input and reach thermal equilibrium at each heat input before measurements are taken.

• Operating in central heating mode is 80°C flow temperature and 60°C return temperature.

• Until the AFCO is equal to 1000ppm, measurements are taken at 20%, 40%, 60%, 70%, 100%, 105%, 110%NB etc..

5.3.1.2. Light Back Test

Lower λ value is provided by the appliance operated at maximum heat input. Light back is be checked according to test conditions given below and λ can be calculated by measuring CO2 by placing an exhaust gas probe in the middle of the HE between two fins.

There is given the fan speed 2150 rpm for RSF appliances in the operating conditions part of this procedure in order to compare different designs, which can cause light back. This speed is not a requirement of EN standard. It was defined in Bosch for this project.

"Light Back Test Procedure" is defined below:

- 1m vertical flue is used for OF appliances and 0.5m horizontal flue is used for RSF appliances (with a fan speed 2150 rpm).
- The appliance is operated at the maximum heat input on the reference gas.
- When thermal equilibrium is reached with the desired return temperature, the operation is controlled, and it is checked whether light back occurs or not.

5.3.1.3. Flame Lift Test

While the appliance has been operating at minimum, the primary air ratio becomes its highest value. If the primary aeration ratio increases, flame velocity decreases. Therefore, flame velocity is at the lowest value, when the appliance is operated at minimum; and it is probable to be observed flame lift problem on the combustion surface.

"Flame Lift Test Procedure" is defined below:

- 1m vertical flue is used for OF appliances and 0.5m horizontal flue is used for RSF appliances (with a fan speed 2150 rpm).
- All tests are carried out twice, with the boiler at ambient temperature and at thermal equilibrium.
- The appliance is operated at the minimum heat input on the test gas.
- The occurrence of flame lift is checked.

5.3.2. Special Tests

In addition to the standard tests, there are specially performed tests for each design in order to check some important parameters clearly. These parameters are temperature and pressure drop for lamella burner fin deck. The tests are called as special tests, and their procedures are determined for the fin deck designs.

5.3.2.1. Temperature Tests

There are some regions on the lamella burner fin deck, where the temperature distribution is important and should be kept under a level during the operation. Because of this, it is needed to check the temperatures on these regions.

In temperature tests, there are used two different types of measurement equipment as being temperature indicating liquids and thermocouples. Both the two methods were used to find the temperature distribution on the frame, collar, and fin bottoms. The temperature indicating liquids are additionally used to define the temperature interval on the fin tips.

"Temperature Test Procedure" is defined below.

- The thermocouple should be rolled up carefully and fixed on the required surface.
- The appliance is operated in central heating mode with 80°C flow temperature and 60°C return temperature.
- The appliance is operated at the maximum heat input.
- The appliance must be operated 20 minutes more after it reaches thermal equilibrium.
- The average of the measured temperatures in 20 minutes after the thermal equilibrium is assumed as the measured temperature by the thermocouple.

5.3.2.2. Pressure Drop Test

Pressure drop is a physical property of LBR fin deck, which influences the flame structure and primary air ratio, λ. Therefore, it is able to apply pressure drop test to compare the characteristics of different fin deck designs.

There is a relationship between the pressure difference and flow velocity as:

$$\Delta P = k \frac{v^2}{2} \tag{5.5}$$

If pressure differences are defined in different velocities, a pressure drop curve will be obtained. Therefore, it will be easy to know the pressure drop in the LBR fin deck for any gas velocities.

"Pressure Drop Test Procedure" is defined below.

- Fin deck to be tested is placed in the pressure drop test rig.
- Air flow is provided by a fan. Fan is operated at different powers.
- The flow velocities are measured for each fan power.
- The pressure differences between the flows before and after fin deck are read in air-pro for each flow velocity.
- Pressure drop curve (air velocity verses pressure difference) is drawn using the test results.

5.4. Test Matrixes

In the entire test matrixes, there are type of appliance, type of the using gas and the performed test number shown pointing out the sample type of the fin deck for each performed test.

Additionally, since this study is a collection - evaluation study of the test results, some tests, which results are used in this master study, had been already performed in development department before this study started.

Combustion curve test, temperature (using thermocouples) test matrixes, NOx test, light back test and flame lift test are shown in Table 5.9, 5.10, 5.11, 5.12 and 5.13, respectively. Pressure drop test was performed for serial, 5004-1 and 5006-1 samples.

Table 5.9. Combustion curve test matrix.

Appliance	Using Gas	Test No.	Fin Deck				
			serial	5004-1	5006-1	5004-2	5006-2
RSF	Natural Gas	serial.RSF.NG	X				
		5004-1.RSF.NG		X			
		5006-1.RSF.NG			X		
		5004-2.RSF.NG				X	
		5006-2.RSF.NG					X
	LPG	serial.RSF.LPG	X				
		5004-1.RSF.LPG		X			
		5006-1.RSF.LPG			X		
		5004-2.RSF.LPG				X	
		5006-2.RSF.LPG					X
OF	Natural Gas	serial.OF.NG	X				
		5004-1.OF.NG		X			
		5006-1.OF.NG			X		
		5004-2.OF.NG				X	
		5006-2.OF.NG					X
	LPG	serial.OF.LPG	X				
		5004-1.OF.LPG		X			
		5006-1.OF.LPG			X		
		5004-2.OF.LPG				X	
		5006-2.OF.LPG					X

Table 5.10. Temperature test matrix.

Test No.	Fin Deck				
	serial	5004-1	5006-1	5004-2	5006-2
serial.RSF.NG	X				
5004-1.RSF.NG		X			
5006-2.OF.NG					X

Table 5.11. NOx test matrix.

Appliance	Using Gas	Test No.	Fin Deck				
			serial	5004-1	5006-1	5004-2	5006-2
RSF	Natural Gas	serial.RSF.NG	X				
		5006-2.RSF.NG					X

Table 5.12. Light back test matrix.

Appliance	Using Gas	Test No.	Fin Deck				
			serial	5004-1	5006-1	5004-2	5006-2
OF	G222	5006-2.OF.NG					X
	G32	5006-2.OF.LPG					X
RSF	G222	5006-2.RSF.NG					X
	G32	5006-2.RSF.LPG					X

Table 5.13. Flame lift test matrix.

Appliance	Using Gas	Test No.	Fin Deck				
			serial	5004-1	5006-1	5004-2	5006-2
OF	G23	5006-2.OF.NG					X
	G31	5006-2.OF.LPG					X
RSF	G23	5006-2.RSF.NG					X
	G31	5006-2.RSF.LPG					X

CHAPTER 6

TEST RESULTS AND DISCUSSION

There were totally 5 sample tested as being 1 serial and 4 new design samples. The test results of the samples were compared with the serial deck and the most preferred sample was defined as optimized one according to that comparison.

The comparison order of the tests was defined in order to decide clearly the most preferred sample. After every test, the sample(s) with worst result(s) was (were) eliminated. Therefore, not every test was performed for every sample as it can be seen in the test matrixes at the end of the previous chapter. This test order is as following.

- Pressure Drop Test
- Temperature Test
- Combustion Performance Curve Test
- NOx Test
- Light Back-Flame Lift Tests

6.1. Pressure Drop Test Results

The pressure drop test was performed for serial, 5004 -1 and 5006 -1 samples. There was no need to define the pressure drop for welded samples (5004-1, 5006-2), since it is clear that they have nearly similar pressure drop with their unwelded ones.

In serial fin deck, which has 1mm fin thickness, pressure drop is bigger then the samples, which have 0.6 mm fin thickness. The difference between two samples is the fin heights. All of the fins in sample 5004 are at the same height. As for sample 5006, its fins are installed with the groups of one long two short fins. Results of two samples show that the fin heights do not affect the pressure drop.

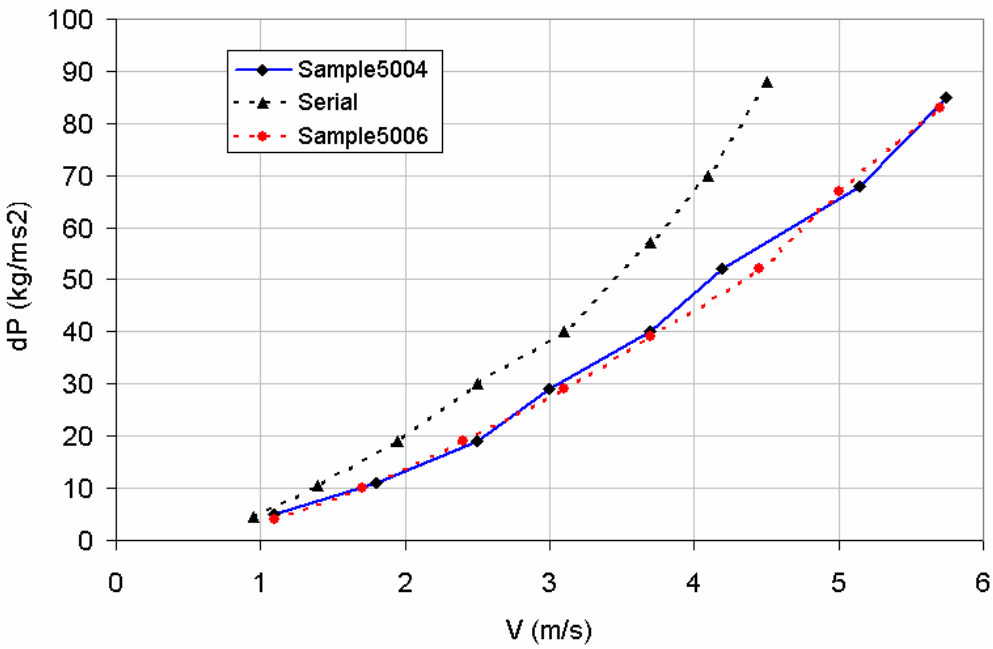

Figure 6.1. Pressure drop curves for different fin deck samples.

To find the pressure drop in **serial 24 kW LBR** fin deck for the gas flow rate of 2857.14dm^3/h, ν is calculated as below:

$$CH_4 + 2\ O_2 + 7.56\ N_2 \rightarrow CO_2 + 2H_20 + 7.56\ N_2 \qquad (5.1)$$

For $\lambda = 1.20$

$$CH_4 + 2\ O_2 + 7.56\ N_2 + 0.4\ O_2 + 1.512\ N_2 \rightarrow CO_2 + 2H_20 + 7.56\ N_2 + 0.4\ O_2 + 1.512\ N_2 \qquad (5.2)$$

$V' = 2857.14 + 2.4 * 2857.14 + 9.072 * 2857.14 = 33034.25$ dm^3/h $= 9.176$ dm^3/s

$V' = \nu * A$, where V'= volumetric flow rate

ν = volumetric velocity

A = open surface

The flow velocity for the **serial** deck is calculated as:

$\nu = 9.176 * 10^{-3}$ (m^3/s) / $(1.6643 * 10^{-2})$ (m^2)

$\nu = 0.551$ m/s

The difference between serial and sample flow velocities is their open surfaces. The velocities will be same for the **sample 5004** and **sample 5006** and calculated as:

$\nu = 9.176 * 10^{-3}$ (m^3/s) / ($1.8702 * 10^{-2}$) (m^2)

$\nu = 0.491$ m/s

Since the pressure drop curve based on the experiment covers only the velocities between nearly 1-4.5 m/s for the serial LBR fin deck, the power trendline of the curve is drawn.

Finally, pressure drops of the serial and sample decks are found from the power trendlines. Extrapolation shows that the pressure drops in serial, 5004 and 5006 samples are nearly as followings.

Serial	$\Delta P \approx 1.76$ kg /ms^2
Samples 5004	$\Delta P \approx 1.2$ kg /ms^2
Samples 5006	$\Delta P \approx 1.0$ kg /ms^2

It was expected before that there is a significant pressure drop in fin deck and hence the combustion process is influenced from pressure drop. These results show the pressure drop in every fin deck design is very low, which can not affect the combustion processes, however, the pressure drop in new samples are lower than the pressure drop in the serial deck. As a result, there is no sample eliminated after the evaluation of the pressure drop test results.

6.2. Temperature Test Results

In Chapter 3, it was mentioned about how important the frame temperature is for a fin deck design. It is clear that welding is most important application for serial deck frame. The fin sides in the 5004-1 and 5006-1 samples was bended and touched to the frames in order to provide heat transfer from frames to the fins without any welding processes. In this test, the frame temperatures of serial, one unwelded sample (5004-1) and one welded sample (5006-2) were measured.

The measured points are shown in Figure 6.2 and this test was performed using thermocouples. The measured temperatures are shown in Table 6.1.

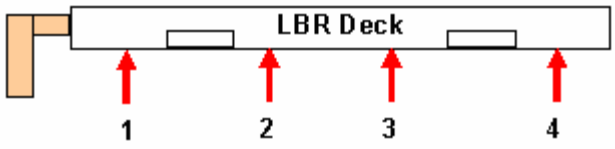

Figure 6.2. Thermocouple locations on the fin deck (front side).

Table 6.1. Frame temperature results (^{o}C).

Sample	**1**	**2**	**3**	**4**
Serial	128,4	131,7	132,5	132,7
5004-1	140,7	160	144,4	163,7
5006-2	78,5	95,9	110,7	101,7

The above results show the sample produced without welding (5004-1) has the highest temperature distribution on the frame. It means that the bended fins are not enough to reduce the frame temperature. Therefore, all the unwelded samples (5004-1, 5006-1) are eliminated in this test.

6.3. Combustion Curve Test Results

Combustion curve test is one of the most important tests for each new design, since their AFCO values and CO curves will be compared with the serial deck. The sample(s) with significantly worse result(s) than the serial deck will be eliminated.

This test was performed for all samples, since it was the first test done in this project. The tests eliminated after the temperature tests are noted in remarks (Table 6.2). There are two different combustion curve test result matrixes. The measurements are taken in the first matrix (Table 6.2) in the flue pipe, in the second matrix (Table 6.3) over the heat exchanger. The sample with unacceptable AFCO value and CO curve is defined according to the result matrix, where the measurements are taken in the flue

pipe (Figure 6.3). Testing over heat exchanger is not a must, but it gives the results from the undiluted exhaust as additional information especially for OF appliances.

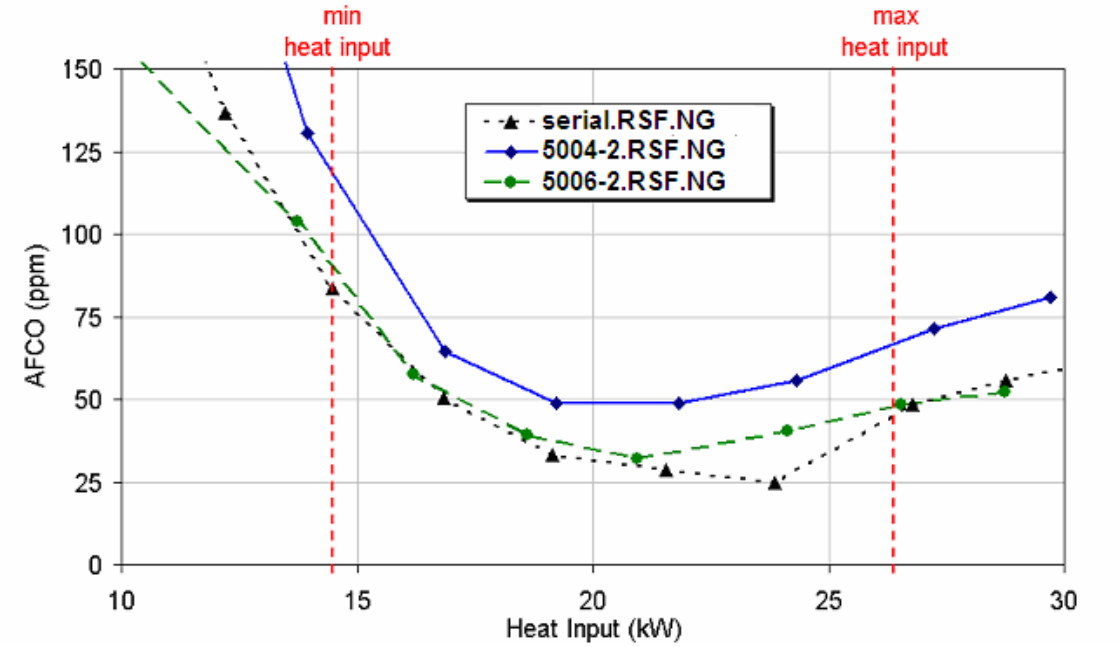

Figure 6.3. Air free CO curves of serial deck, 5004-2 and 5006-2 samples according to the results of the tests performed using natural gas in RSF appliances (in the flue pipe).

According to the test result matrix for measurements taken in flue pipe (Table 6.2); the AFCO values and CO curves of the sample 5004-2 are unacceptable for RSF appliances using natural gas. All the AFCO values and the CO curves of the sample 5006-2 are nearly the same with the serial sample or better than it. Because of this and with the help of the results (Table 6.3), which tests were performed by taking the measurements over the heat exchanger, 5004-2 sample is eliminated after the combustion curve test.

Table 6.2. Combustion Test Results (measurements were taken in the flue pipe)

Appliance	Using Gas	Test No.	Fin Deck					Combustion Curve Test Results								Remarks
										In flue pipe						
			serial	5004-1	5006-1	5004-2	5006-2	Burner pressure	Heat Input	NO	CO	CO2	λ	AF-NOx	AF-CO	
								mbar	kW	ppm	ppm	%	-	ppm	ppm	
RSF	Natural Gas	serial.RSF.NG	X					15,7	26,78	10,10	22,60	5,46	2,14	21,64	**48,43**	
		5004-1.RSF.NG		X				15,7	25,97	9,50	26,90	5,40	2,17	20,58	58,28	eliminated before
		5006-1.RSF.NG			X			15,7	26,40	2,20	22,80	5,79	2,02	4,45	46,07	eliminated before
		5004-2.RSF.NG				X		15,7	27,25	6,90	26,70	4,37	2,68	18,47	**71,49**	**worst**
		5006-2.RSF.NG					X	15,7	26,53	6,00	23,50	5,65	2,07	12,42	48,66	
	LPG	serial.RSF.LPG	X					36,5	26,37	10,70	36,40	6,78	2,06	22,09	75,16	
		5004-1.RSF.LPG		X				36,5	26,11	12,70	33,00	5,85	2,39	30,39	78,97	eliminated before
		5006-1.RSF.LPG			X			36,5	26,85	3,20	21,50	6,94	2,02	6,46	43,37	"
		5004-2.RSF.LPG				X		36,5	26,78	10,60	30,20	5,49	2,55	27,03	77,01	
		5006-2.RSF.LPG					X	36,5	26,50	12,10	23,30	6,90	2,03	24,55	47,28	
OF	Natural Gas	serial.OF.NG	X					13,4	27,47	8,40	33,20	5,16	2,27	19,05	75,28	
		5004-1.OF.NG		X				13,4	28,27	13,80	26,60	5,17	2,26	31,23	60,20	eliminated before
		5006-1.OF.NG			X			13,4	28,14	6,20	19,10	5,21	2,25	13,92	42,89	eliminated before
		5004-2.OF.NG				X		13,4	27,40	18,20	31,50	5,06	2,31	42,08	72,84	
		5006-2.OF.NG					X	13,4	26,80	6,90	17,80	5,10	2,29	15,83	40,84	
	LPG	serial.OF.LPG	X					36,5	26,75	6,50	21,40	5,90	2,37	15,42	50,78	
		5004-1.OF.LPG		X				36,5	27,49	9,70	23,20	5,97	2,35	22,75	54,41	eliminated before
		5006-1.OF.LPG			X			36,5	27,04	3,20	15,00	5,82	2,41	7,70	36,08	eliminated before
		5004-2.OF.LPG				X		36,1	26,72	20,00	20,80	5,60	2,50	50,00	52,00	
		5006-2.OF.LPG					X	36,5	27,65	6,80	17,30	6,18	2,27	15,40	39,19	

Table 6.3. Combustion Test Results (measurements were taken over the heat exchanger)

Appliance	Using Gas	Test No.	Fin Deck					Combustion Curve Test Results							
			serial	5004-1	5006-1	5004-2	5006-2	Burner pressure	Heat Input	Over HE					
										NO	CO	CO2	λ	AF-NO	AF-CO
								mbar	kW	ppm	ppm	%	-	ppm	ppm
RSF	Natural Gas	serial.RSF.NG	X					15,7	26,78	19,50	36,30	10,86	1,08	21,01	39,11
		5004-1.RSF.NG		X				15,7	25,97	19,30	42,50	9,60	1,22	23,52	51,80
		5006-1.RSF.NG			X			15,7	26,40	22,00	20,70	10,41	1,12	24,73	23,27
		5004-2.RSF.NG				X		15,7	27,25	20,70	52,60	9,69	1,21	24,99	**63,51**
		5006-2.RSF.NG					X	15,7	26,53	11,50	27,20	9,60	1,22	14,02	33,15
	LPG	serial.RSF.LPG	X					36,5	26,37	18,00	43,80	11,98	1,17	21,04	51,19
		5004-1.RSF.LPG		X				36,5	26,40	23,90	52,10	11,64	1,20	28,75	62,66
		5006-1.RSF.LPG			X			36,5	26,85	22,50	54,10	11,54	1,21	27,30	65,63
		5004-2.RSF.LPG				X		36,5	26,78	18,00	43,80	11,98	1,17	21,04	51,19
		5006-2.RSF.LPG					X	36,5	26,50	17,90	29,10	11,34	1,23	22,10	35,93
OF	Natural Gas	serial.OF.NG	X					13,4	27,47	20,30	51,40	10,60	1,10	22,41	56,73
		5004-1.OF.NG		X				13,4	28,27	28,50	56,00	10,36	1,13	32,19	63,24
		5006-1.OF.NG			X			13,4	28,14	14,20	30,40	10,60	1,10	15,67	33,55
		5004-2.OF.NG				X		13,4	27,40	39,40	73,40	10,38	1,13	44,41	**82,73**
		5006-2.OF.NG					X	13,4	26,80	19,70	44,00	10,55	1,11	21,85	48,80
	LPG	serial.OF.LPG	X					36,5	26,75	15,20	31,20	11,97	1,17	17,78	36,49
		5004-1.OF.LPG		X				36,5	27,49	19,30	41,60	11,22	1,25	24,08	51,91
		5006-1.OF.LPG			X			36,5	27,04	9,00	16,30	11,49	1,22	10,97	19,86
		5004-2.OF.LPG				X		36,1	26,72	35,90	53,50	11,37	1,23	44,20	**65,88**
		5006-2.OF.LPG					X	36,5	27,65	11,70	18,30	11,92	1,17	13,74	21,49

6.4. NOx Test Results

NOx test were performed for serial and 5006-2 samples in order to define the NOx level of serial and 5006-2 samples and compare them. Air free NOx curves were also plotted according to the results of the combustion tests for these two samples. The NOx value of the sample 5006-2 is better than the value of serial deck according to the test results in Table 6.4. NOx class of the sample 5006-2 is the 5th alike the serial deck.

Table 6.4. NOx test results.

Appliance	Using Gas	Fin Deck					NOx (mg/kWh)	NOx Class
		serial	5004-1	5006-1	5004-2	5006-2		
RSF	Natural Gas	X					9	5
						X	7	5

In Figure 6.4, the air free NOx curves of these two samples also show their NOx levels in details.

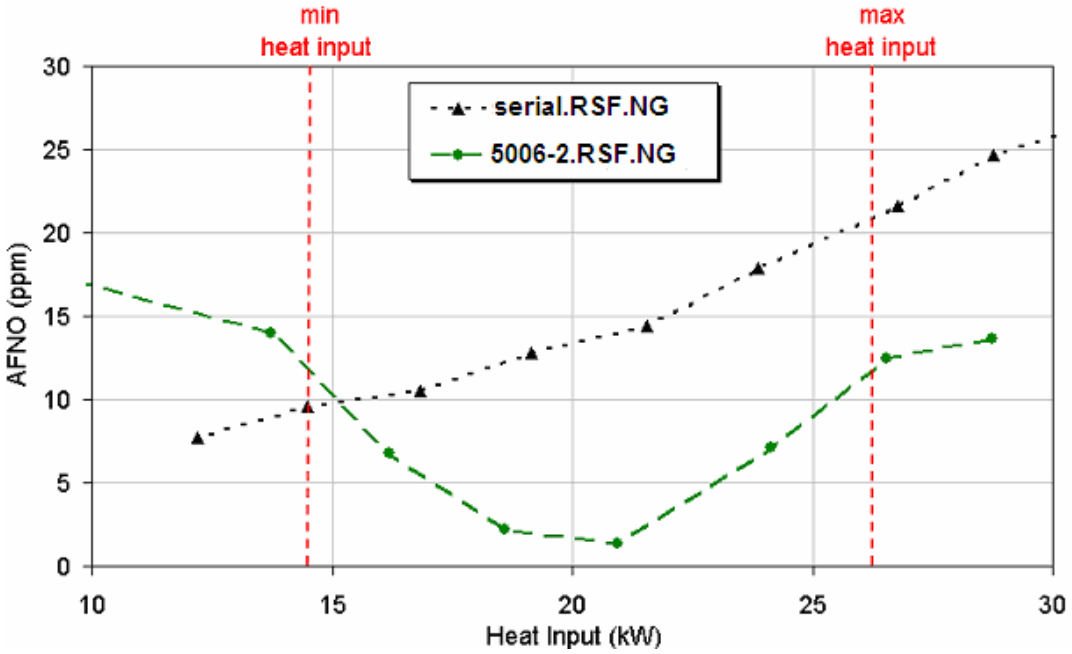

Figure 6.4. Air free NO_x curves of serial deck and the sample 5006-2 according to the results of the tests performed using NG in RSF appliances (in the flue pipe).

6.5. Light Back and Flame Lift Test Results

Light back and flame lift test is performed for serial and 5006-2 sample. It has been already known the serial deck has no light back and flame lift problem. It was checked again. The light back and flame lift tests was important for 5006-2, since if there will be a problem it could not be acceptable. A s a result, no light back and no flame lift occur in the tests of 5006-2 (Table 6.5).

Table 6.5. Light back and flame lift test results.

Appliance	Appliance	Using Gas	Fin Deck					Result
			serial	5004-1	5006-1	5004-2	5006-2	
Light Back	OF	G222					X	No
		G32					X	No
	RSF	G222					X	No
		G32					X	No
Flame Lift	OF	G23					X	No
		G31					X	No
	RSF	G23					X	No
		G31					X	No

6.6. Discussion on the Test Results

Test results of each sample are compared with the results of serial fin deck to determine whether the samples perform similar to or better than serial fin deck or not. According to the test results, some of the samples are eliminated, if they had even one worse result than serial deck, and one passed from all tests (Table 6.6).

Table 6.6. Comparison of the test results

	5004-1	5004-2	5006-1	5006-2
Performed Tests				
Pressure Drop Test	ok	ok	ok	ok
Temperature Test	**failed**	ok	**failed**	ok
Combustion Curve Test		**failed**		ok
NOx Test				ok
Light Back Test				ok
Flame Lift Test				ok

After the temperature test, the samples 5004-1 and 5006-1 are eliminated. This decision are made according to the measured frame temperatures of the sample 5004-1. Its max frame temperature is higher than that of the serial deck, since its frame is not welded to the fins. Frame temperature at high values causes damages on the sealing, therefore this design becomes unacceptable. The sample 5006-1 is also unwelded, therefore it is also eliminated.

The sample 5004-2 is eliminated after the combustion curve test because of its CO-values. CO emissions are inevitable products of incomplete combustion as being mentioned about in Chapter 1. In the same chapter, it is also mentioned that only about a third of the unburned hydrocarbons are found in exhaust as fuel molecules and the rest results CO production. For the sample 5004-2, the reason of its high CO formation should be that there is much more unburned gas in its exhaust. And unburned gas rates are related with flame stability, since when flames are unstable, gas can not burn completely and unburned mixture can pass trough. Therefore, the layout and design parameters related with the flame stability should be evaluated to find the reason of the high CO rates in the sample 5004-2.

The layout parameters, which influence the flame stability, are primary aeration ratio-λ, laminar flame velocity-S_L and mixture velocity-$v_{mixture}$ (Table 3.4). In table 5.3, λ values of the samples 5004-2 and 5006-2 are shown, and it is seen that they are very close to each other. If these values are assumed equal, there are two parameters left, S_L and $v_{mixture}$, influenced flame stability.

The flame velocity-S_L values of the sample 5004-2 and 5006-2 can be compared by evaluating the layout parameters, which influence S_L (Table 3.4). There are three layout parameters as being flame temperature, mixture temperature and primary aeration ratio. It is seen that the λ values are nearly the same in Table 6.3. The differences in other two parameters are also neglected, since the tests are performed under the same operating conditions (cause of the close mixture temperatures) and have close burner heat inputs (related to close flame temperatures).Therefore, the flame velocities for all of the samples are assumed as the same.

To evaluate the mixture velocities, it is necessary to check the fin deck design parameters. Since designs of the other burner parts and the operation conditions are the same for all of the samples, the gas/air mixtures should be at the same speed just before passing through the each fin deck. However, the fin heights in the sample 5004-2 are different from the fin heights in the sample 5006-2. This geometry difference causes

some local differences on the mixture flows and temperature distributions on the fin deck surfaces. These geometrical effects cause some local changes in the mixture velocity distributions (just after passing through each fin deck), while the average mixture velocities for these samples, which have the same open surface areas, stay equal. According to the geometrical effects, in the sample 5006-2, the local flow velocities should be closer to the flame velocity than that in the sample 5004-2 is. In the other words, the flames in 5006-2 are more stable than the flames in 5004-2 (Figure 3.14). Therefore the unburned gas molecules and hence the CO formation in exhaust are the highest ones in the sample 5004-2.

CHAPTER 7

MODELING AND SIMULATION

In Chapter 6, it is proposed that different amounts of CO molecules measured in 5004-2 and 5006-2 fin deck combustion curve tests are based on the effect of their geometry differences on the unburned gas mass fraction. The unburned gas mass fractions are investigated for both geometries by performing 2D simulation using Fluent 6.0 software. Computational area and the boundary conditions of two fin decks are shown in Figure 7.1.

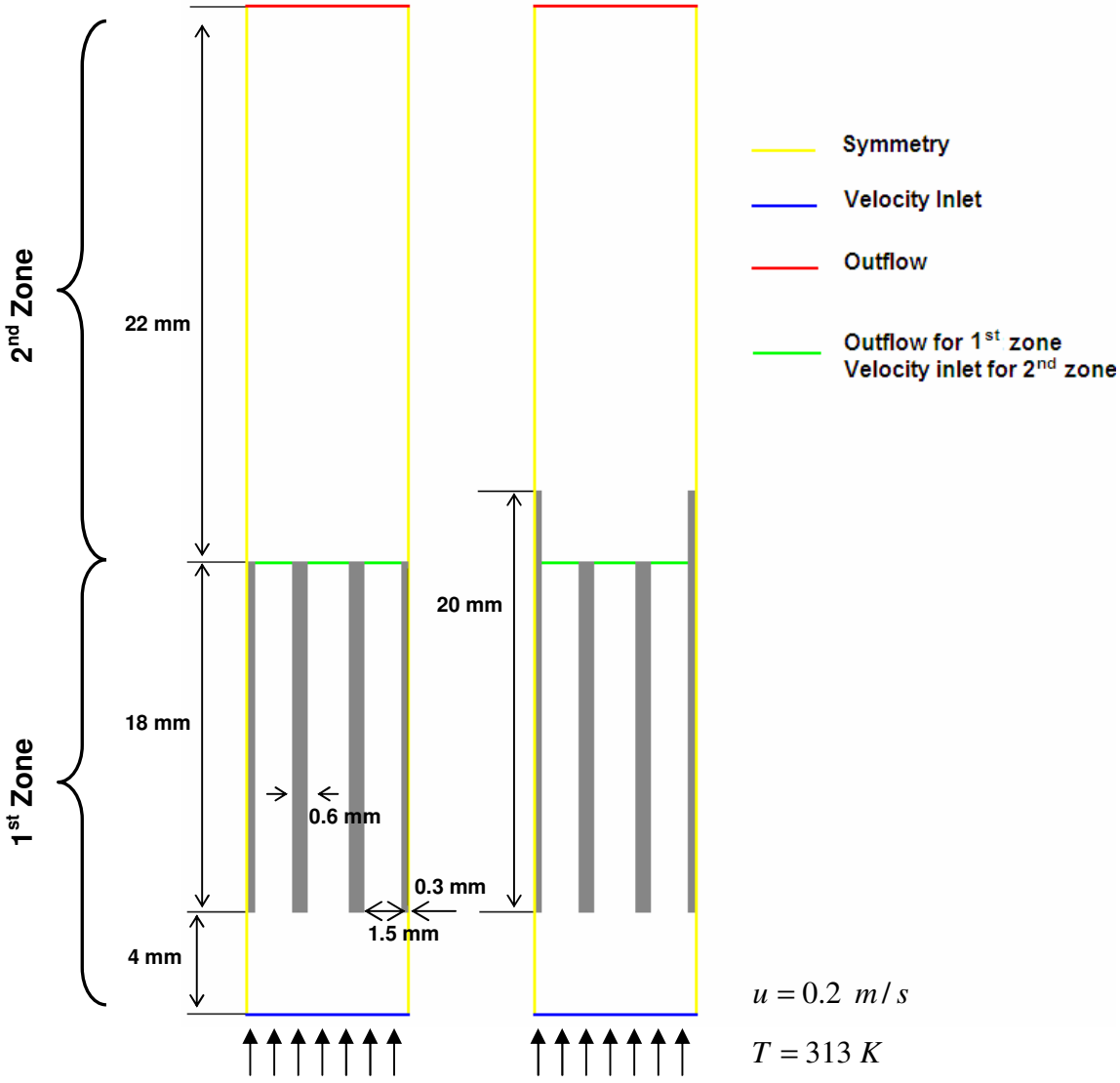

Figure 7.1. Computational areas and boundary conditions of the sample 5004-2 (on the left-hand-side) and the sample 5006-2 (on the right-hand-side).

The computation areas are divided into two zones. In the first zone, mixture flow is investigated and outlet velocity distribution is defined. These outlet velocities are used to determine the inlet velocities of the mixture flow into the second zone, where the combustion occurs.

7.1. Governing Equations

A finite-volume method is used to discretize the 2D continuity, momentum, energy and species conservation equations in the fluid, shown below (Fluent 2002).

Continiuty
$$\frac{\partial \rho}{\partial t} = -\left[V_x \frac{\partial \rho}{\partial x} + V_y \frac{\partial \rho}{\partial y} + \rho\left(\frac{\partial V_x}{\partial x} + \frac{\partial V_y}{\partial y}\right)\right] \tag{7.1}$$

Momentum
$$\frac{\partial}{\partial t}(\rho V_x) = -\left[\frac{\partial(\rho V_x V_x)}{\partial x} + \frac{\partial(\rho V_x V_y)}{\partial y}\right] - \frac{\partial p}{\partial x} + \frac{\partial \tau_{xx}}{\partial x} + \frac{\partial \tau_{yx}}{\partial y} \tag{7.2}$$

$$\frac{\partial}{\partial t}(\rho V_y) = -\left[\frac{\partial(\rho V_x V_y)}{\partial x} + \frac{\partial(\rho V_y V_y)}{\partial y}\right] - \frac{\partial p}{\partial y} + \frac{\partial \tau_{xy}}{\partial x} + \frac{\partial \tau_{yy}}{\partial y} \tag{7.3}$$

Energy
$$\frac{\partial}{\partial t}(\rho h) = -\left[\frac{\partial(\rho h V_x)}{\partial x} + \frac{\partial(\rho h V_y)}{\partial y}\right] + \frac{\partial\left(k_f \frac{\partial T}{\partial x}\right)}{\partial x} + \frac{\partial\left(k_f \frac{\partial T}{\partial y}\right)}{\partial y} + \sum_i \left[\frac{\partial\left(h_i \rho D_{i,m} \frac{\partial Y_i}{\partial x}\right)}{\partial x} + \frac{\partial\left(h_i \rho D_{i,m} \frac{\partial Y_i}{\partial y}\right)}{\partial y}\right] - \sum_i h_i R_i \tag{7.4}$$

Species
$$\frac{\partial}{\partial t}(\rho Y_i) = -\left[\frac{\partial(\rho Y_i V_x)}{\partial x} + \frac{\partial(\rho Y_i V_y)}{\partial y}\right] + \frac{\partial\left(\rho D_{i,m} \frac{\partial Y_i}{\partial x}\right)}{\partial x} + \frac{\partial\left(\rho D_{i,m} \frac{\partial Y_i}{\partial y}\right)}{\partial y} + R_i \tag{7.5}$$

In above equations, V_x and V_y are velocities in x and y directions. P is static pressure, and h shows enthalpy. $D_{i,m}$ is the diffusion coefficient for species i in mixture, and k_f shows the conductivity of fluid.. Y_i is the local mass fractions of each species and R_i is the mass rate of creation or depletion by chemical reaction. τ represents the stress tensor described as in the equation (7.6), where μ is the molecular viscosity.

$$\tau_{ij} = \mu\left(\frac{\partial V_i}{\partial x_j} + \frac{\partial V_j}{\partial x_i}\right) \tag{7.6}$$

7.2. Chemical Reaction

Fully premixed methane/air mixtures with λ=1.2 excess air are fed into the models. Species mass fractions are needed for the flow and combustion simulations and calculated from combustion equation (7.6) of CH_4 / air mixture for λ=1.2 (selected according to the test results of RSF appliances using natural gas shown in Table 5.3).

$$CH_4 + 1.2a\,(O_2 + 3.76\,N_2) \longrightarrow CO_2 + 2\,H_2O + 0.2a\,O_2 + (1.2 \times 3.76)a\,N_2$$

$$O_2: \quad 1.2a = 1 + 1 + 0.2a \longrightarrow a = 2$$

$$CH_4 + 2.4\,(O_2 + 3.76\,N_2) \longrightarrow CO_2 + 2\,H_2O + 2.4\,O_2 + 9.024\,N_2 \tag{7.6}$$

$$\text{Mass fraction of } CH_4: \frac{16.043\,\text{kg/kmol}}{16.043\,\text{kg/kmol} + 2.4*(31.999 + 3.76*28.013)\,\text{kg/kmol}} = 0.0464$$

$$\text{Mass fraction of } O_2: \frac{2.4*31.999\,\text{kg/kmol}}{16.043\,\text{kg/kmol} + 2.4*(31.999 + 3.76*28.013)\,\text{kg/kmol}} = 0.2222$$

7.3. Boundary Conditions

Schematic view of two computational domains is shown in Figure 7.1. These domains are divided into two zones. There are four types of boundaries as being inlet, outlet, solid surface and symmetry. Velocity magnitude is considered as 0.2 m/s for the inlet boundary of the first zone. In the second zone, velocity magnitudes are defined using the first zone results. Flow temperature is 313 K for both inlet boundaries for first and second zones. For the solid surfaces velocities are zero, where surface temperature is defined as 303 K. For symmetry boundaries velocity is zero in x direction, where the equation (7.7) is valid for the velocity in y direction and temperatures. Velocities in x and y directions and temperatures defined in the equation (7.8) for the outlet boundaries.

$$\frac{\partial V_Y}{\partial x} = \frac{\partial T}{\partial x} = 0 \tag{7.7}$$

$$\frac{\partial V_x}{\partial y} = \frac{\partial V_y}{\partial y} = \frac{\partial T}{\partial y} = 0 \tag{7.8}$$

7.4. Modeling and Simulation of the First Zone

First zone conditions are assumed as being the same for two fin deck models. Therefore, one 2D model is prepared and mashed in GAMBIT for the mixture flow simulation of both 5004-2 and 5006-2 models. Interval size of each mash is 0.1 mm (Figure 7.2). Conservation equations are solved to simulate steady-state, laminar mixture flow using segregated solution solver.

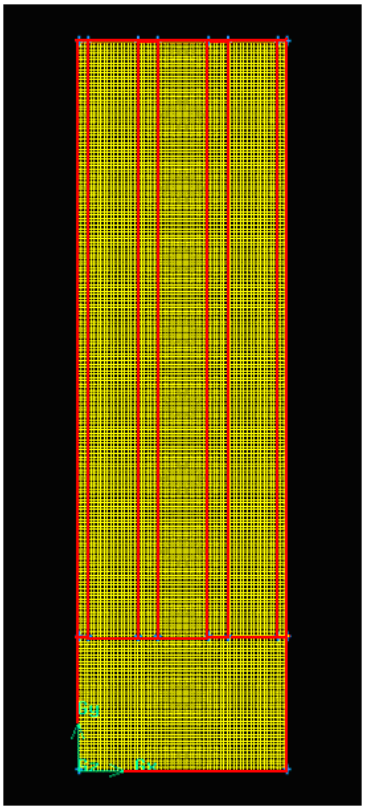

Figure 7.2. 2D mashed model of the first zone.

Material types of fluid and solid faces in the first zone defined as methane/air mixture and steel, respectively. Material properties of methane/air mixture and steel are shown in Table 7.1.

Table7.1. Material properties of methane/air mixture and steel.

Material Property		Methane/Air Mixture	Steel
Density	**(kg/m3)**	incompressible-ideal-gas	8030
Cp	**(j/kgK)**	mixing-law	502.48
Thermal Conductivity	**(W/mK)**	0.0454	16.27
Viscosity	**(kg/ms)**	1.72e-05	
Mass Diffusivity	**(m2/s)**	2.88e-05	

7.4.1. Obtained Results in the First Zone Simulation

Velocity distribution of gas/air mixture through the fins is defined after continuity converged and shown in Figure 7.3.

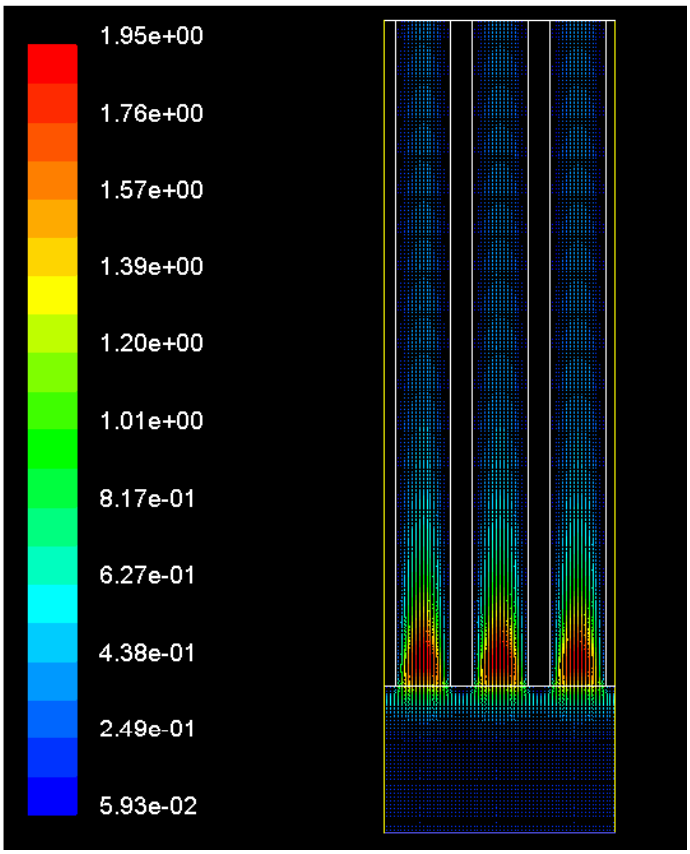

Figure 7.3. Velocity distribution of gas/air mixture through the fins in the first zone.

Velocity magnitudes for each mash in outlet flow boundary (Figure 7.4) are noted in order to use them as inlet mixture velocities in second zone (Table 7.2).

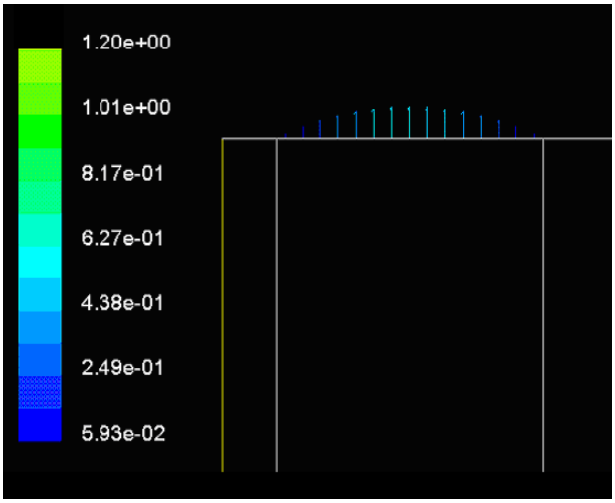

Figure 7.4. Velocity vectors of outlet flow boundaries of the fist zone.

Table 7.2. Velocity magnitudes for each mash in one outlet flow boundary.

Exit number	1	2	3	4	5	6	7	8	9	10	11	12	13	14	15
Outlet Velocity (m/s)	0,06	0,06	0,154	0,25	0,25	0,34	0,34	0,34	0,34	0,34	0,25	0,25	0,154	0,06	0,06

7.5. Modeling and Simulation of the Second Zone

Second zones of the fin deck models 5004-2 and 5006-2 are created and mashed in Gambit 6.0. In these combustion zone inlets, 15 edges are drawn between each fin in order to be able to input different velocity magnitudes shown as outlet velocity magnitudes in Table 7.3 (Figure 7.5). Models, materials and boundary condition values of two fin deck combustion zones are defined in Fluent 6.0 solver.

Solver, viscous model, energy and species model definitions are identified in the definition of models section. Segregated solver is defined for 2D space. In viscous model and energy definitions, standard k-epsilon model and energy equation are chosen. Mixture material, volumetric reaction and therefore turbulence-chemistry interaction sections are defined after the definition of species transport model.

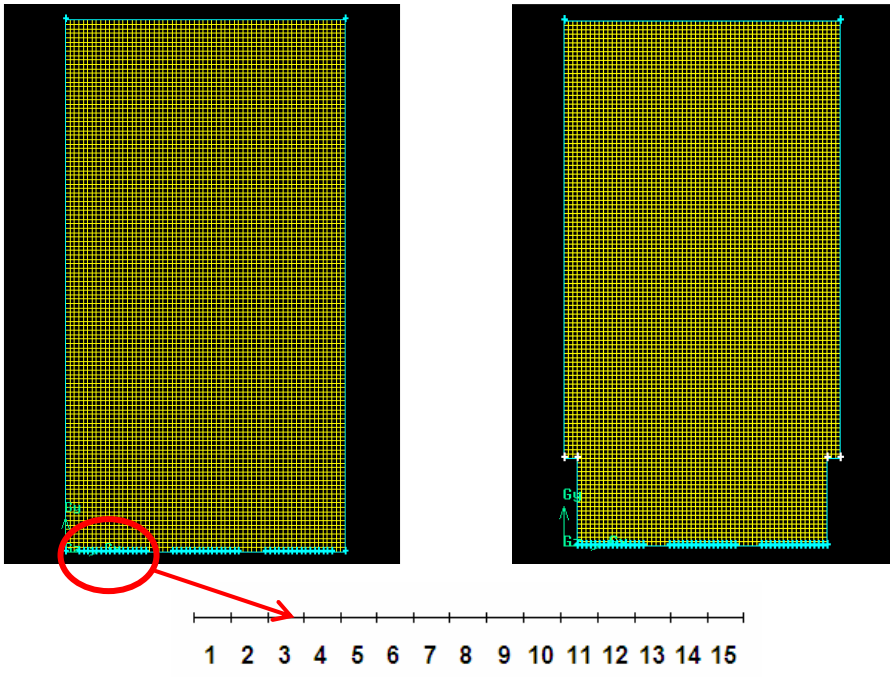

Figure 7.5. Velocity inlet entries for the model 5004-2 (on the left-hand-side) and the model 5006-2 (on the right-hand-side)

Methane-air and steel properties are established in the definition of materials section as shown in Table 7.1. In the boundary condition definitions; inlet velocities, outflow, wall and symmetry conditions are determined. In the velocity-inlet settings; velocity magnitudes, temperature and species mass fractions are defined. Inlet velocities are specified from the first zone solution. Inlet velocity settings of each entry are shown in the Table 7.3.

Table 7.3. Velocity inlet settings for the models 5004-2 and 5006-2.

	Velocity magnitude (m/s)	Hydraulic diameter (m)	Temperature (K)	CH4 mass fraction	O2 mass fractions
Entry 1	0,06	0.5e-5	313	0,0464	0,2222
Entry 2	0,06	0.5e-5	313	0,0464	0,2222
Entry 3	0,154	0.5e-5	313	0,0464	0,2222
Entry 4	0,25	0.5e-5	313	0,0464	0,2222
Entry 5	0,25	0.5e-5	313	0,0464	0,2222
Entry 6	0,34	0.5e-5	313	0,0464	0,2222
Entry 7	0,34	0.5e-5	313	0,0464	0,2222
Entry 8	0,34	0.5e-5	313	0,0464	0,2222
Entry 9	0,34	0.5e-5	313	0,0464	0,2222
Entry 10	0,34	0.5e-5	313	0,0464	0,2222
Entry 11	0,25	0.5e-5	313	0,0464	0,2222
Entry 12	0,25	0.5e-5	313	0,0464	0,2222
Entry 13	0,154	0.5e-5	313	0,0464	0,2222
Entry 14	0,06	0.5e-5	313	0,0464	0,2222
Entry 15	0,06	0.5e-5	313	0,0464	0,2222

Fin tips in each model are defined as wall type boundary conditions. Steel is selected as the material of fins. Temperatures of related edges are calculated using following equations (7.7) and (7.8), which have been formulated from the measurements of fin temperatures of serial fin deck (Parmantier et al. 2003).

$$T_{long}(x) = 0.0505x^3 - 0.3635x^2 + 5.9189x + 68.301 \quad (7.7)$$

$$T_{short}(x) = 0.002x^4 - 0.0296x^3 + 0.0777x^2 + 1.4468x + 94.597 \quad (7.8)$$

In the model 5004-2, fin tip temperature is calculated using the equation of long fins (7.7) for x=18 mm. In the model 5006-2, fin tip temperature of long fins is calculated using the same equation for x=20 mm. In this model, fin tip temperature of

short fins is calculated using the equation of short fins (7.8) for x=18 mm. There are also inner fin faces in the model 5006-2. Temperature of these faces is calculated from fallowing equation.

$$T_{innerface} = \frac{T_{long}(20) - T_{long}(18)}{2} \tag{7.4}$$

Wall type boundary condition settings for each fin zones are shown in Table 7.4.

Table 7.4. Wall type boundary condition settings for fin zones

	Temperature (K)
5004-2 fin tips	625
5006-2 long fin tips	718
5006-2 short fin tips	456
5006-2 long fin inside faces	671

After all boundary conditions of the fin tips are determined, the initial temperature of each simulation zone is defined as 1200 K in order to provide ignition.

7.5.1. Obtained Results in the Second Zone Simulation

Velocity distribution, temperature distribution and CH_4 mass fraction of 5004-2 and 5006-2 combustion zones are displayed in the Figure 7.6, 7.7 and 7.8, respectively.

It is seen from Figure 7.6; geometrical differences between the fin deck models affect the velocity distributions. For the model 5004-2, it is observed that velocity profile becomes quickly linear after passing through the fins. Since the shear stresses are significant near the inner surfaces of long fins, a boundary layer velocity profile is observed between the long fins in the combustion zone of the model 5006-2.

The flame temperatures are shown in Figure 7.7. According to the temperature distribution in the model 5004-2, it can be said that flames in this model have flat flame shape. Since the long fins give additional cooling effect to the combustion zone of the model 5006-2, these flames have a typical flame shapes, where the highest temperature occurs in the middle.

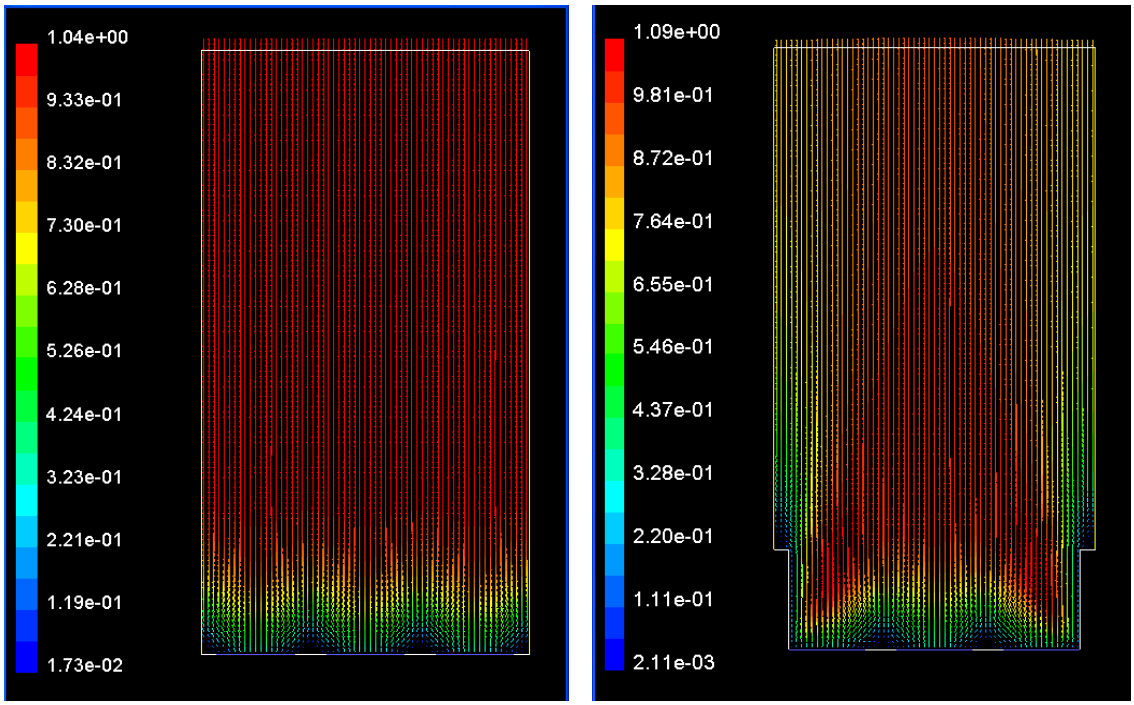

Figure 7.6. Velocity distribution in exhaust of the model 5004-2 (on the left-hand-side) and the model 5006-2 (on the right-hand-side).

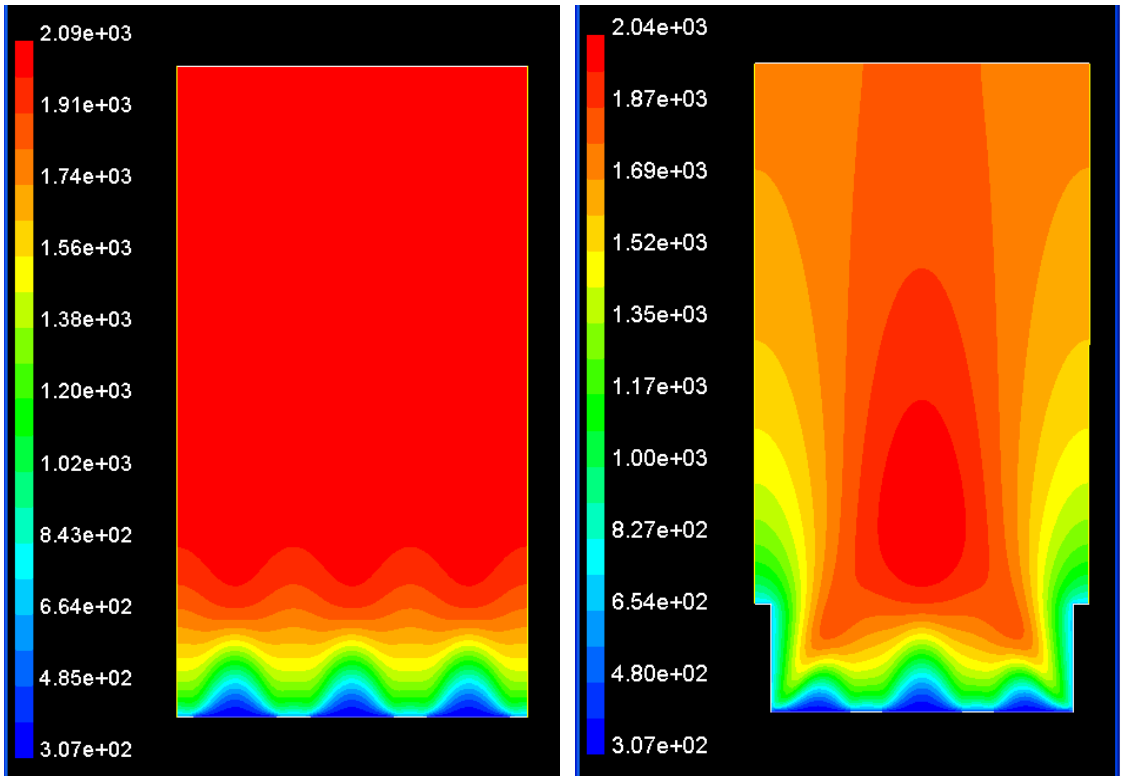

Figure 7.7. Temperature distribution in exhaust of the model 5004-2 (on the left-hand-side) and the model 5006-2 (on the right-hand-side).

The methane mass fractions of the models 5004-2 and 5006-2, which mean the unburned gas mass fractions in exhaust, are shown in Figure 7.8. The methane mass fractions are quickly decreases after passing through the fins. It is clearly seen the reduction rate of the methane mass fraction is increasing near the long fins in the model 5006-2. However, mass fractions decreases equally in the model 5004-2 with a highest rate observed in the model 5006-2. Therefore total unburned gas mass fraction is higher in 5004-2 than that in 5006-2.

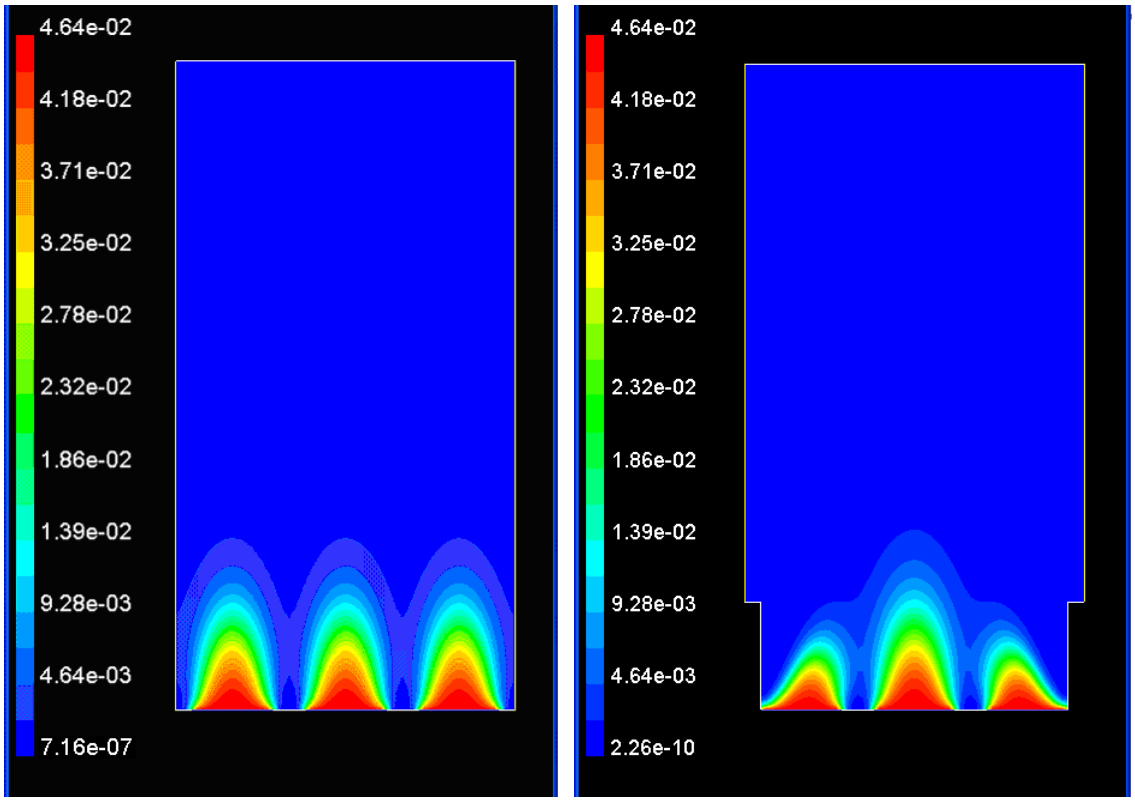

Figure 7.8. CH_4 mass fraction in exhaust of the model 5004-2 (on the left-hand-side) and the model 5006-2 (on the right-hand-side)

CHAPTER 8

CONCLUSIONS

The lamella burner fin deck, which surface is the combustion surface of the burner, is one of the main components of the low-emission lamella burner. In this study, fin deck is analyzed according to the combustion characteristics, and four new samples are developed. Each sample is tested to check whether it is performing similar to or better than the serial fin deck or not. After the experimental analysis, the most preferred sample was defined as the optimized fin deck sample.

In this study, gas combustion, layout and design parameters of fin deck are investigated in Chapter1 – 4. After the performed tests, the samples are evaluated according to their test results and some of them are eliminated. In the evaluation of test results, investigations about gas combustion, layout and design parameters of fin deck are discussed to explain theoretically whether the fin deck samples are preferable or not.

After the experiments, sample 5006-2 is only the one which passed from five performance tests. In the modeling and simulation section of this study, combustion zones of passed sample 5006-2 and failed sample 5004-2 are compared according to their combustion curve test results. The difference between these samples is their fin geometries. These different geometries have different influences on the flame stability and cause different unburned gas fractions in exhausts. According to the theoretical background, different CO values measured in combustion curve test of these two fin deck samples are based on these different unburned gas quantities. Therefore, unburned gas mass fractions in exhaust for two different fin deck models are simulated, and the comparison with the CO values measured in combustion curve tests are used for verification.

2D models of the combustion zones of fin deck samples 5004-2 and 5006-2 are created in Gambit 6.0 and exported to the Fluent 6.0. Another 2D model, which simulates the flow distribution through the fins, is created to define the velocity inlet boundary conditions of these combustion models. Mixture temperatures are assumed as 313 K, and fin tip temperatures are calculated from the formulas derived in another study about lamella burner (Parmantier et al. 2003).

The two combustion zone models are run and iterated until the flame temperatures and CH_4 mass fractions are converged. According to the simulations, fin deck model 5004-2, which has higher air-free CO values measured in combustion curve test, has also higher CH_4 mass fraction in its exhaust than fin deck model 5006-2 has (Table 8.1).

Table 8.1. AF-CO and CH4 mass fractions of the samples 5004-2 and 5006-2 form test and numerical simulation results.

	Experimental Results	Numerical Results
Sample No	**AF-CO**	**CH4 Mass Fraction**
5004-2	*63,51 ppm*	*7.16 e-7*
5006-2	*33,15 ppm*	*2.26 e-10*

CH_4 mass fraction is found higher in the simulation of the combustion zone model 5004-2 than in the numerical analysis of the model 5006-2 as proposed according to its high measured AF-CO values in the combustion curve test.

For the numerical analysis, the computational areas were divided into two zones. In the first zone temperature of the fins were assumed as 313K neglecting the affect of the combustion on fin temperatures. In reality, the fin temperatures and velocity distributions of the mixture flows are influenced from combustion. Neglecting this effect can be acceptable since the two models have been compared under the same conditions in the second zone. However, dividing the computational areas into two zones can be the cause of the high flame temperature on the outflow layer of the fin deck model 5004-2. The average temperature on the outflow layer of the fin deck model 5006-2 is nearer to the real flame temperatures, since the cooling effect of the long fins is included in the combustion simulation more effectively.

The reason of dividing the computational areas into two zones is the impossibility to simulate the combustion over the fin tips using the species transport model in Fluent 6.0. Since the fully premixed methane/air mixture is fed into the model under the fin bottoms, mixture starts to burn before passing through the fins. However, it is understood that if the computational zone can be solved as a single area covering both the first and the second zones using a sufficient solver; the cooling effect of the fins can be simulated better to define flame temperature in the fin deck model 5004-2

and even 5006-2. In that case, mixture flow velocities will be affected from combustion including radiation; therefore the simulations will come closer to the reality.

After all of the investigations and evaluations, the sample 5006-2, with the fin thickness 0.6 mm and the fin distribution as being one long and two short, was determined as the most preferred fin deck design in this study, which is about the lamella burner fin deck optimization.

REFERENCES

Braack, M. and Rannacher, R. 1999. "Adaptive Finite Element Methods for Low-Mach-Number Flows with Chemical Reactions", 30th Computational Fluid Dynamics, Lecture Series von Karman Institute, Belgium, Vol. 3, pp. 1-93.

Cerbe, G., 1999. *Grundlagen der Gastechnik,* (Carl Hanser Verlag, München).

Chen, Y.C. and Bilger, R.W. 2000. "Stabilization Mechanisms of Lifted Laminar Flames in Axisymmetric Jet Flows", *Elsevier, Combustion and Flame*, Vol. 123, pp.23-45.

Chou, C., Chen, J., Yam C.G. and Marx, K.D. 1998 "Numerical Modeling of NO Formation in Laminar Bunsen Flames—A Flamelet Approach", *Elsevier, Combustion and Flame*, Vol. 114, pp. 420-435.

Dugger, G.L., Weast, R.C. and Heimel, S. 1955 "Effect of Preflame Reaction on Flame Velocity of Propane-Air Mixtures", 5th Symp. (Internat.) on Combustion, Reinhold Pub. Corp., New York, pp. 589-595.

Dupont, V. and Williams, A. 1998. "NO_x Mechanisms in Rich Methane-Air Flames", *Elsevier, Combustion and Flame*, Vol. 114, pp. 103-118.

Fine, B. 1958. "The Flashback of Laminar and Turbulent Burner Flames at Reduced Pressure", *Elsevier, Combustion and Flame*, Vol. 2, pp. 253-266.

Fluent 2002. "Fluent 6.0", Lebanon.

Gaydon A.G. and Wolfhard H.G., 1970. *Flames*, (Chapman & Hall, London), p. 12.

Jensen, W.B. 2005. "The Origin of the Bunsen Burner", *Journal of Chemical Education*, Vol. 82 No. 4.

Jones, H.R.N. and Leng, J. 1996. "The Influence of Fuel Composition on Emissions of CO, NO, and NO_2 from a Gas-Fired Pulsed Combustor", *Elsevier, Combustion and Flame*, Vol. 104, pp. 419-430.

Kanury, A.M., 1975. *Introduction to Combustion Phenomena*, (Gordon & Breach Science Pub, NY).

Kuo, K.K., 1986. *Principles of Combustion,* (John Willey & Sons, Canada).

Kurz, P.F. 1957. "Some Factors Influencing Stability Limits of Bunsen Flames", *Elsevier, Combustion and Flame*, Vol. 1, pp. 162-178.

Lammers, F.A. and de Goey, L.P.H. 2003. "A numerical study of flash back of laminar premixed flames in ceramic-foam surface burners", *Elsevier, Combustion and Flame*, Vol. 133, pp. 47-61.

Lee, S.T. and T'ien, J.S. 1982. "A Numerical Analysis of Flame Flashback in a Premixed Laminar System", *Elsevier, Combustion and Flame*, Vol. 48, pp. 273-285.

Naha, S. and Aggarwal, S.K. 2004. "Fuel Effects on NOx Emissions in Partially Premixed Flames", *Elsevier, Combustion and Flame*, Vol. 139, pp. 90-105.

Nishioka, M., Ishigami, Y., Horii, H.; Umeda, Y. and Nakamura Y. 2006. "NOx Reduction Mechanism of a Methane–Air Smithells Flame", *Elsevier, Combustion and Flame*, Vol. 147, pp. 93-107.

Parmantier, S., Braack M., Riedel U. and Warnatz J. 2001. "Modellierung und Simulation eines Lamellenbrenners", Interdisziplinaeres Zentrum für Wissenschaftliches Rechnen Ruprecht – Karls - Universität Heidelberg, p. 29.

Parmantier, S., Braack M., Riedel U. and Warnatz J. 2003. "Modeling of Combustion in a Lamella Burner", *Taylor & Francis, Combust. Sci. and Tech.,* Vol. 175, pp. 185-206.

Plothe, M. and Sönmezışık F. 2003. "Lamella Burner Report", Bosch Thermotechnologies Development Report, Manisa, pp. 5-39.

Robson, K. and Wilson M.J.G. 1969. "The Stability of Laminar Diffusion Flames of Methane", *Elsevier, Combustion and Flame*, Vol. 13, pp. 626-634.

Schalla, R.L., Clark, T.P. and McDonald G.E. 1954. "Formation and Combustion of Smoke in Laminar Flames", *NACA Reports*, Report 1186, pp. 657-677.

Smithells, A. and Ingle, H. 1892. "The Structure and Chemistry of Flames", *J. Chem Soc.* 61, pp. 204-16.

Tecce, L., Continillo, G. and Marra, F.S. 2005. "Lean Laminar Premixed Flame Quenching Investigation in Parallel Plates Arrester", *Proceedings of 7th Italian Conference on Chemical and Process Engineering*, Italia, Vol. 1, pp. 557-562.

The European Standard EN 297:1994, 2003. "Gas-fired central heating boilers - Type B11 and B11BS boilers fitted with atmospheric burners of nominal heat input not exceeding 70 kW", BSI, British Standards.

The European Standard EN 483:2000, 2002. "Gas-fired central heating boilers - Type C boilers of nominal heat input not exceeding 70 kW", BSI, British Standards.

Turns, S.R., 2000. *An Introduction to Combustion: Concepts and Applications,* (McGraw-Hill, New York).

WEB_1, 1996. NEWPORT Homepage, 10.07.2005. http://www.newport.com/servicesupport/Tutorials/default.aspx?id=82

WEB_2, 2000. Nitrogen oxides emissions standards for domestic gas appliances, 01.06.2005. http://www.deh.gov.au/atmosphere/airquality/publications/index.html

WEB_3, 2003. Burner History, 15/04/2005. http://www.process-heating.com/CDA/ArticleInformation/EnergyNotesItem/0,3271,90695,00.html

WEB_4, 2003. Gaseous Combustion Kinetics, 01.06.2005. http://www.abo.fi/~ezabetta/

Zel'dovich, Y.B., Frank-Kamenetsky, D.A. and Semenov, N. 1938. "Comprehensive Theory", Compt. Rend. Acad. Sci., USSR, Vol. 19, p. 693.